

One-Body Properties and their Perturbative Accuracy with Aufbau Suppressed Coupled Cluster Theory

Conor Bready,¹ Harrison Tuckman,¹ and Eric Neuscamman^{1,2, a)}

¹⁾*Department of Chemistry, University of California, Berkeley, California 94720, USA*

²⁾*Chemical Sciences Division, Lawrence Berkeley National Laboratory, Berkeley, CA, 94720, USA*

(Dated: 20 March 2026)

We derived and implemented the calculation of the one-body reduced density matrix for Aufbau suppressed coupled cluster theory, from which excited state natural orbitals and one-body properties, like atomic populations and dipole moments, are obtained. We utilized the natural orbitals to refine the ASCC solution for simple valence and Rydberg systems, exploring the process of repeatedly solving the ASCC equations in successive natural orbital bases to achieve independence from the starting molecular orbitals. For dipole moments in small molecules where high-level comparison data is available, we find that the accuracy of ASCC essentially matches that of linear response and equation-of-motion coupled cluster as long as care is taken to preserve the response’s perturbative completeness.

I. INTRODUCTION

The proper manipulation of electronic excited states to perform intended chemical tasks requires knowledge of both the necessary excitation energy and the characteristic properties of the desired state. Many linear response-based methods such as time dependent density functional theory (TD-DFT)^{1–3} and equation of motion coupled cluster theory (EOM-CC)^{4–6} are able to provide both energies and properties quite accurately.^{7–9} However, these linear response methods, unlike state-specific methods, are dependent upon the proper behavior of the ground state, which has the potential to be problematic when the excited state’s optimal geometry is far from that of the ground state’s.^{10,11} Approaches such as the spin-flip method for both TD-DFT^{12,13} and EOM-CC,^{14,15} or double ionization potential and double electron affinity for just EOM-CC,^{16–21} help ameliorate the problems that arise due to this multi-configurational character while still maintaining a single-reference formalism; however, this requires chemical knowledge that the newly chosen reference must itself remain well-behaved at the interested geometry. On the other hand, Aufbau suppressed coupled cluster (ASCC)²² provides a state-specific approach, bypassing the reliance that a different potential energy surface still yields reasonable results. Furthermore, ASCC maintains all of the benefits of coupled cluster theory (CC), providing an interesting candidate for the evaluation of excited state properties. After some adjustments informed by extending the perturbative analysis performed by Tuckman et al.²³ to property evaluations, we demonstrate that ASCC’s response can be just as accurate as other excited state CC counterparts, with the potential to be more accurate for charge transfer systems where ASCC has previously excelled.²⁴

In addition to the benefits of state-specific methods when exploring structures outside of their optimal ground

state geometries, these methods also have the benefits of orbital relaxations tailored to the excited state itself. Many approaches utilize this concept of trying to optimize the excited state orbitals, including various methods in DFT,^{25–42} CASSCF,^{43–48} CI,^{49–56} perturbation theory,^{57–59} CC,^{60–65} variational Monte Carlo,^{66–77} and more. Likewise, ASCC was recently shown to benefit from its intrinsic orbital relaxations by demonstrating near independence from the reference provided.⁷⁸ Generically, utilizing state-specific orbitals often results in a more accurate description of the excited state itself and is therefore incredibly valuable when comparing to experiments. Derivatives of this accurate energy expression with respect to one-body perturbations will yield density matrices, from which key properties can be extracted. Examples of such properties include information about the locations and magnitudes of charge and spin,^{79–81} electronic dipole and other higher order multipole moments,^{82,83} and even magnetic moments,^{83–85} all of which have the potential to be compared against experimental results collected from various types of pump-probe spectroscopy.^{86–88} While the method of finite difference can be used to calculate any of these derivatives, whether it be through the direct application of an external field or just modification of the one-electron integrals in the Hamiltonian to yield the one-body reduced density matrix (1-RDM), analytic derivatives benefit from improved speed and robustness.^{89–91} The true barrier to obtaining these accurate properties typically lies instead in the theoretical derivation, which becomes increasingly complex as the energy expression itself grows in intricacy.

With all of this in mind, we aim to add to ASCC the functionality of one-body property calculations that can be evaluated through the 1-RDM. This first requires a theoretical derivation of the working equations to solve for ASCC’s response. As one might expect, we find that the response equations closely resemble those of ground state coupled cluster.^{92,93} However, upon completing a perturbative analysis of this response, key differences appear that require ASCC to be considerably more careful when deciding which amplitudes to in-

^{a)}Electronic mail: eneuscamman@berkeley.edu

clude. We therefore test multiple amplitude inclusion approaches informed by perturbative correctness of the 1-RDM via properties. First, we investigate whether a fully reference-independent solution can be found by iteratively using ASCC’s natural orbitals (NOs) as the orbital starting point for new ASCC calculations. We next compare excited state Mulliken and Löwdin population analyses on various charge transfer systems, one of which where EOM-CCSD has been shown to perform poorly,^{24,57} demonstrating ASCC’s reliability in more difficult systems. Finally, we use the highly accurate QUEST database^{94,95} to compare excited state dipole moments between ASCC, EOM-CC, and linear response CC (LR-CC).^{96–102}

II. THEORY

A. ASCC Lagrangian

ASCC was designed with the goal of creating an excited-state-specific method that maintains cost-parity with single-reference ground-state coupled cluster theory while retaining all of its benefits: size consistency, size extensivity, accurate correlation energies, and systematic improvability. Additionally, when dealing with excited states, size intensivity for excitation energies was also desired. With all of these in mind, the ASCC ansatz was formulated as

$$|\Psi_{\text{ASCC}}\rangle = e^{-\hat{S}^\dagger} e^{\hat{T}} |\phi_0\rangle \quad (1)$$

where \hat{S}^\dagger is a de-excitation operator, \hat{T} is an excitation operator, and $|\phi_0\rangle$ is the Aufbau determinant, often coming from closed-shell Hartree-Fock.²² The objective of the new exponentiated de-excitation operator is to either partially or completely cancel out the Aufbau determinant through the term $-\hat{S}^\dagger \hat{T} |\phi_0\rangle$ in the Taylor series expansion of Equation (1), which excites and then de-excites back to the original determinant, but with negative contribution.²²

Utilizing this ansatz, we can proceed similar to ground state coupled cluster to formulate expressions for the excited state energy and amplitude equations. The energy equation will correspond to the expectation value of the doubly similarity transformed Hamiltonian with respect to the formal reference, $|\phi_0\rangle$, and the amplitude equations to the projections onto excited determinants $|\mu\rangle$, which can be used to optimize the \hat{T} amplitudes. These can be represented concisely through the definition of an ASCC Lagrangian, where enforcing stationarity with respect to the Lagrange multipliers, λ_μ , yields the amplitude equations.

$$\begin{aligned} \mathcal{L}_{\text{ASCC}} = & \left\langle \phi_0 \left| e^{-\hat{T}} e^{\hat{S}^\dagger} \hat{H} e^{-\hat{S}^\dagger} e^{\hat{T}} \right| \phi_0 \right\rangle \\ & + \sum_{\mu} \lambda_{\mu} \left\langle \mu \left| e^{-\hat{T}} e^{\hat{S}^\dagger} \hat{H} e^{-\hat{S}^\dagger} e^{\hat{T}} \right| \phi_0 \right\rangle \end{aligned} \quad (2)$$

This Lagrangian is nearly identical to that of the ground state, with the only difference coming from the similarity transform of the Hamiltonian with \hat{S}^\dagger . While there are other CC methods that utilize multiple similarity transforms, such as transcorrelated CC or extended CC, these other methods focus on improving the accuracy of the ground state.^{103–105} On the other hand, the purpose of the second similarity transform in ASCC is to ensure that the Aufbau contribution to the wavefunction is suppressed, thus allowing it to target the desired excited state. By continuing to follow the techniques used for the ground state Lagrangian, we can define a new $\hat{\Lambda}$ operator that closely resembles the \hat{T} operator, but excites the bra instead of the ket. We use i, j, \dots to denote occupied molecular orbitals, a, b, \dots virtual molecular orbitals, and w, x, \dots any molecular orbital.

$$\hat{\Lambda} = \hat{\Lambda}_1 + \hat{\Lambda}_2 + \dots + \hat{\Lambda}_N \quad (3)$$

$$\hat{\Lambda}_n = \left(\frac{1}{n} \right)^2 \sum_{ij\dots ab\dots}^n \lambda_{ij\dots}^{ab\dots} \hat{i}^\dagger \hat{j}^\dagger \dots \hat{b} \hat{a} \quad (4)$$

Putting this together with Equation (2) yields an even more concise Lagrangian.

$$\mathcal{L}_{\text{ASCC}} = \left\langle \phi_0 \left| \left(1 + \hat{\Lambda} \right) e^{-\hat{T}} e^{\hat{S}^\dagger} \hat{H} e^{-\hat{S}^\dagger} e^{\hat{T}} \right| \phi_0 \right\rangle \quad (5)$$

If one was solely interested in the ASCC energy, enforcing stationarity of $\hat{\Lambda}$ would be sufficient. However, if one instead desired any properties, one would ideally want stationarity of the Lagrangian with respect to every parameter.¹⁰⁶ Just as in the ground state theory, enforcing stationarity with respect to \hat{T} also provides values for $\hat{\Lambda}$.⁹² Thus, after these stationarity conditions are met, the remaining nonzero terms in the presence of a perturbation consists of the response of \hat{S}^\dagger , the response of the molecular orbital coefficients from the reference of choice, and the response of the Hamiltonian itself. In this preliminary study, we restrict our excited states to those defined purely by a single configuration state function (CSF); as defined in previous works, this results in \hat{S}^\dagger taking the form of

$$\hat{S}_{1\text{-CSF}}^\dagger = \frac{1}{\sqrt{2}} \left(\hat{h}_\downarrow^\dagger \hat{p}_\downarrow + \hat{h}_\uparrow^\dagger \hat{p}_\uparrow \right) \quad (6)$$

with h and p representing the “hole” and “particle” orbitals, respectively. The subspace that \hat{S}^\dagger acts in will be referred to as the primary subspace, as this represents the orbitals where the electronic excitation primarily occurs. Conveniently, the coefficient of \hat{S}^\dagger here is constant, implying that the term containing the response of \hat{S}^\dagger in the 1-CSF case will be 0. We recognize that this definition leads to an ansatz that looks very similar to that of two determinant CC (TD-CC). However, ASCC and TD-CC differ in their nonlinear terms and perturbative completeness (discussed more in Section II B) due to the additional similarity transformation from \hat{S}^\dagger , resulting in differing energies.^{107–109} Furthermore, ASCC

is more generalizable than TD-CC, as it can describe excited states with more than 1 CSF and it can describe doubly excited states through only minor modifications of coefficients and initial guesses.¹⁰⁹

In ground state CC, the response of the molecular orbitals to the perturbation is often ignored when specifically calculating one-body properties. This is because CC's own orbital relaxations on top of the reference reduce the significance of the additional molecular orbital response term.^{110,111} In EOM- and LR-CC, the effects of orbital relaxation are more impactful since the orbitals aren't optimized for excited states. However, including additional cluster operators mitigates these effects due to the correlation method itself performing better orbital relaxations, resulting in a smaller dependence on the original orbital's response.^{5,95,112} Conversely, as ASCC already allows for significant state-specific orbital relaxation similar to ground state CC, we expect the effects of explicitly including the orbital response to be comparable in magnitude to that of the ground state. For this reason, and because issues related to perturbative completeness are likely more impactful (see Section IIB), we opt to ignore this small contribution in the present study. We also note that, because each state gets its own orbital relaxations, the ASCC excited state wave functions will not be exactly orthogonal to each other or to the ground state, which is common in state-specific theories. So long as the ansatz is accurate for the states being studied, the degree of this non-orthogonality should be small.

Under these approximations, enforcing stationarity with respect to $\hat{\Lambda}$ and \hat{T} within the 1-CSF framework leads to the result that a perturbation with respect to any parameter χ can be represented as

$$\frac{\partial \mathcal{L}_{\text{ASCC}}}{\partial \chi} = \left\langle \phi_0 \left| \left(1 + \hat{\Lambda} \right) e^{-\hat{T}} e^{\hat{S}^\dagger} \frac{\partial \hat{H}}{\partial \chi} e^{-\hat{S}^\dagger} e^{\hat{T}} \right| \phi_0 \right\rangle \quad (7)$$

which again closely parallels the ground state CC Lagrangian when also neglecting the orbital response. One can separate out the coefficients of the Hamiltonian's response projected into the molecular orbital basis from the rest of the expression to create useful definitions for the one- and two-body unrelaxed reduced density matrices (1- and 2-RDM).

$$\gamma_{wx}^{\text{ASCC}} = \left\langle \phi_0 \left| \left(1 + \hat{\Lambda} \right) e^{-\hat{T}} e^{\hat{S}^\dagger} \hat{w}^\dagger \hat{x} e^{-\hat{S}^\dagger} e^{\hat{T}} \right| \phi_0 \right\rangle \quad (8)$$

$$\Gamma_{wxyz}^{\text{ASCC}} = \left\langle \phi_0 \left| \left(1 + \hat{\Lambda} \right) e^{-\hat{T}} e^{\hat{S}^\dagger} \hat{w}^\dagger \hat{x}^\dagger \hat{z} \hat{y} e^{-\hat{S}^\dagger} e^{\hat{T}} \right| \phi_0 \right\rangle \quad (9)$$

Additionally, it can be seen from these that the energy expression can be evaluated simply by taking the product of the Hamiltonian with the 1- and 2-RDM and summing over all indices, shown in Equation (10). Furthermore, it follows from Equation (7) that the response of the energy to a perturbation looks nearly identical to the regular energy expression when utilizing the density matrices, with the only difference being the use of the perturbed

Hamiltonian.

$$E_{\text{ASCC}} = \sum_{wx} \gamma_{wx}^{\text{ASCC}} h_{wx} + \frac{1}{4} \sum_{wxyz} \Gamma_{wxyz}^{\text{ASCC}} \langle wx || yz \rangle \quad (10)$$

$$\frac{\partial E_{\text{ASCC}}}{\partial \chi} = \sum_{wx} \gamma_{wx}^{\text{ASCC}} \frac{\partial h_{wx}}{\partial \chi} + \frac{1}{4} \sum_{wxyz} \Gamma_{wxyz}^{\text{ASCC}} \frac{\partial \langle wx || yz \rangle}{\partial \chi} \quad (11)$$

For one-body properties, the second term in Equation (11) disappears, leaving just the product of the 1-RDM with the perturbed one electron integrals. As mentioned previously though, this result is only the case when the orbital response terms are ignored and the system remains 1-CSF. For references best described by more than one CSF, response of \hat{S}^\dagger would also need to be taken into consideration.

Throughout this entire framework though, the focus has been solely on the right-hand eigenvectors of the Hamiltonian and ensuring that the targeted excited state is the one described by the wavefunction. However, if one instead focuses on the left-hand side of the Lagrangian, the theory becomes less straightforward. Here, the \hat{S}^\dagger no longer performs its intended function of suppressing the Aufbau contribution. Instead, due to its exponentiated form, a given n -CSF reference for \hat{S}^\dagger can actually perform a $2n$ -fold excitation within the primary subspace on the bra. While optimization of the left eigenvectors is still achieved through $\hat{\Lambda}$, thus making ASCC bivariational just like ground state CC,¹¹³ the overall effect that \hat{S}^\dagger has on the left-hand side of the wavefunction should still be explored in more depth, especially since it wasn't required for the calculation of energies.

B. Perturbative Analysis

Before we complete a perturbative analysis of the left-hand side of our Lagrangian to determine how \hat{S}^\dagger might alter the accuracy of ASCC's properties, we will first review the perturbative analysis of the cluster operators and Hamiltonian originally outlined by Tuckman et al.²³ We start by examining the ASCC ansatz. In order to achieve the desired zeroth order wavefunction, it must be the case that both \hat{S}^\dagger and some parts of \hat{T} be nonzero at zeroth order. As the coefficient of \hat{S}^\dagger is constant, this implies that it resides exclusively at zeroth order. On the other hand, as any excitations by cluster operators outside of the primary subspace cannot be offset by the de-excitation performed by \hat{S}^\dagger , we can conclude that any fully non-primary cluster amplitudes and mixed amplitudes containing both primary and non-primary indices must be zero at zeroth order, as is the case for ground state CC. While the specific definition of $\hat{T}^{(0)}$ will vary depending on the number of CSFs deemed necessary to describe the excitation, the single CSF case remains quite

simple.

$$\hat{S}_{1\text{-CSF}}^{\dagger(0)} = \hat{S}_{1\text{-CSF}}^{\dagger} \quad (12)$$

$$\hat{T}_{1\text{-CSF}}^{(0)} = \hat{S}_{1\text{-CSF}} - \frac{1}{2} \left(\hat{S}_{1\text{-CSF}} \right)^2 \quad (13)$$

However, this definition by itself can result in undesired consequences. Consider if one were to follow the standard perturbative partitioning of the Hamiltonian, where the zeroth order contribution arises from the block diagonal occupied-occupied and virtual-virtual parts of the Fock matrix, with everything else considered first order. From this, the off-diagonal parts of the zeroth order Hamiltonian can couple with the primary indices of $\hat{T}^{(0)}$ to generate zeroth order mixed amplitudes, which we know from our ansatz should be 0 at zeroth order. Note that, even when working in the canonical Hartree-Fock orbital basis, the Fock matrix is not diagonal, because it is constructed not from the Hartree-Fock 1-body density matrix but from that of the excited state starting point (e.g., the excited CSF). We do expect it to be diagonally dominant, though. Thus, to prevent mixed amplitudes from becoming zeroth order, we instead partition our zeroth order Hamiltonian into four block diagonal pieces,

$$\hat{H}^{(0)} = \sum_{h_1 h_2} f_{h_1 h_2} \hat{h}_1^\dagger \hat{h}_2 + \sum_{ij} f_{ij} \hat{i}^\dagger \hat{j} \quad (14)$$

$$+ \sum_{p_1 p_2} f_{p_1 p_2} \hat{p}_1^\dagger \hat{p}_2 + \sum_{ab} f_{ab} \hat{a}^\dagger \hat{b} \quad (15)$$

$$\hat{H}^{(1)} = \hat{H} - \hat{H}^{(0)}$$

where h and p still refer to hole and particle indices, but now i and j refer to solely non-primary occupied indices and a and b to solely non-primary virtual indices. While this new partitioning of the Hamiltonian breaks invariance to orbital rotations between the hole orbital and other occupied orbitals and between the particle orbital and other virtual orbitals, it retains invariance with respect to rotations within each of the four subspaces (hole, non-primary occupied, particle, and non-primary virtual) individually.²³

With definitions for the perturbative partitioning of the Hamiltonian and the zeroth order portions of \hat{T} , the determination of which cluster amplitudes are nonzero at each order can be achieved. To mirror ground state CCSD, it was decided that the \hat{T} amplitudes to be included in ASCC are those that contribute at first order to the wavefunction. For 1-CSF, those include all singles, doubles, and a slice of the triples that contain at least three primary indices.²³ Note that while this is more than ground state CCSD, due to the primary space scaling as $O(1)$, the worst additional amplitudes scale as $O(N^3)$ in memory and contribute no additional $O(N^6)$ cost terms, thus maintaining asymptotic cost parity. A partially linearized version of ASCC (PLASCC) also uses these same definitions, but with specific non-linear terms removed in an effort to eliminate contributions from terms that would normally be canceled out at higher orders of PT.²³

Upon completion of the perturbative analysis of the Hamiltonian, \hat{S}^\dagger , and \hat{T} for 1-CSF ASCC, we finally have the tools necessary to investigate the left-hand side of the Lagrangian. Here, we find that in order to left project with purely the desired excited state, a zeroth order $\hat{\Lambda}$ described by solely a two-body operator is required (see Appendix).

$$\hat{\Lambda}_{1\text{-CSF}}^{(0)} = - \left(\hat{S}_{1\text{-CSF}}^\dagger \right)^2 \quad (16)$$

In ground state CC, the $\hat{\Lambda}_n$ amplitudes appear at the same order of perturbation theory as the corresponding \hat{T}_n amplitudes. However, as can be seen from the zeroth order contributions alone, this is not true for ASCC, as there is no one-body operator in the zeroth order definition of $\hat{\Lambda}$. In the determination of the first order pieces, we find that $\hat{\Lambda}^{(1)}$ contains all the same respective parts as $\hat{T}^{(1)}$, but also includes the slice of triples containing one primary and two non-primary de-excitations and the slice of quadruples with two primary de-excitations (see Appendix for nonzero quadruples contributions). While the addition of these new slices would not increase the overall asymptotic scaling of ASCC, they would add additional $O(N^6)$ tensor contractions and additional $O(N^4)$ memory requirements beyond what is needed for CCSD.

To test whether these additional terms are worth the effort, we will test the effectiveness of three different choices for which amplitudes to include in \hat{T} and $\hat{\Lambda}$. First, we allow \hat{T} to contain only its amplitudes that receive first order contributions and we restrict $\hat{\Lambda}$ to the same set of mirrored amplitudes (i.e. singles, doubles, and the slice of triples with at least three primary indices). This approach, which we refer to as $\text{ASCC}^{(M,1)}$ and $\text{PLASCC}^{(M,1)}$, leads the theory to contain the same set of $O(N^6)$ ‘‘bottleneck’’ terms that are present in ground state CCSD. Next, we allow \hat{T} and $\hat{\Lambda}$ to each separately contain whichever of their amplitudes receive first order contributions in the amplitude and response equations, respectively, an approach we refer to as $\text{ASCC}^{(1,1)}$ and $\text{PLASCC}^{(1,1)}$. Note that, in this case, there are more amplitudes inside $\hat{\Lambda}$ than there are in \hat{T} , and so the usual approach of defining the amplitude equations as the derivatives of \mathcal{L} with respect to the $\hat{\Lambda}$ amplitudes yields too many equations. Instead, we form the residual equations as usual only for the amplitudes in \hat{T} that have first order contributions (i.e. those present in $\text{ASCC}^{(M,1)}$). We then approximate the remaining amplitudes in \hat{T} , each of which would be second order, by setting them equal to zero. The $\hat{\Lambda}$ amplitudes are then solved for in the standard way: for each amplitude in $\hat{\Lambda}$, we get an equation to solve by setting the corresponding \hat{T} -amplitude-derivative of \mathcal{L} to zero, whether or not we are allowing that \hat{T} amplitude to be nonzero. Finally, we form the $\text{ASCC}^{(1,M)}$ and $\text{PLASCC}^{(1,M)}$ approaches by allowing $\hat{\Lambda}$ to contain any amplitude that receives a first order contribution and then activating the same mirrored set of amplitudes within \hat{T} .

To get a better sense of the significance of omitting

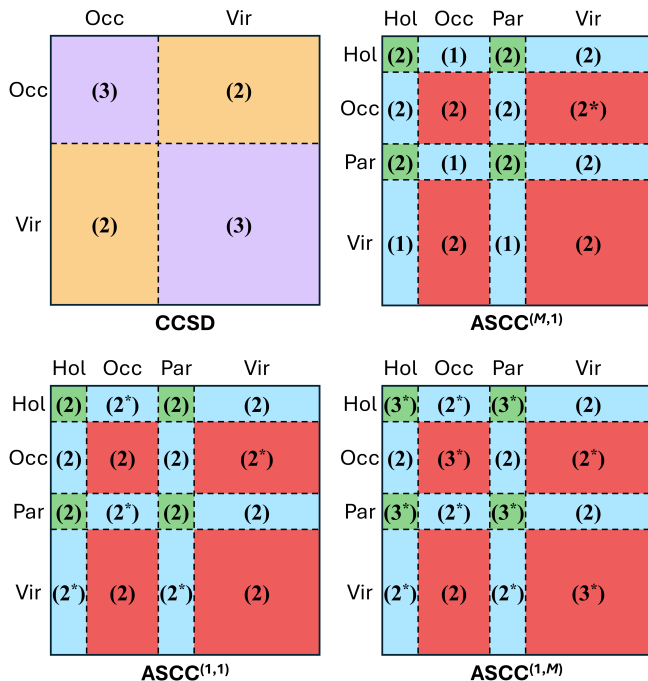


Figure 1. The CCSD and (PL)ASCC 1-RDMs with orders of perturbative correctness indicated. For CCSD, the all occupied and all virtual blocks are highlighted in purple and the occupied-virtual blocks are highlighted in orange. For (PL)ASCC, the all primary blocks are highlighted in green, the mixed blocks in blue, and the all non-primary blocks in red. The * indicates that the block is one order lower with PLASCC (e.g. (3^*) becomes (2) for PLASCC).

various parts of \hat{T} or $\hat{\Lambda}$, we turn our attention to the perturbative correctness of the 1-RDM, shown in Figure 1. In ground state CCSD, the 1-RDM is complete through third order in the occupied/occupied and virtual/virtual blocks, but only second order in the off-diagonal blocks. However, in ASCC^(M,1), the four blocks along the diagonal are now only complete through second order, alongside some, but not all, of the off-diagonal sections. Interestingly, due to the lack of incorporation of the first order $\hat{\Lambda}$, the pattern of perturbative completeness in the off-diagonal sections is not always symmetric. A more in depth analysis depicting this difference between the primary/non-primary occupied blocks (γ_{hi} and γ_{ih}) can be found in the Appendix, Section V A. Upon symmetrization, the 1-RDM becomes Hermitian, with any block taking on the lesser completeness of itself and its adjoint. This results in the all primary and the all non-primary blocks remaining complete through second order, but all mixed blocks being complete through only first order. When additionally including all $\hat{\Lambda}^{(1)}$ pieces, the entirety of the ASCC^(1,1) 1-RDM becomes complete through second order, demonstrating improvement, but still not to the level of the ground state. Finally, for ASCC^(1,M), the perturbative completeness

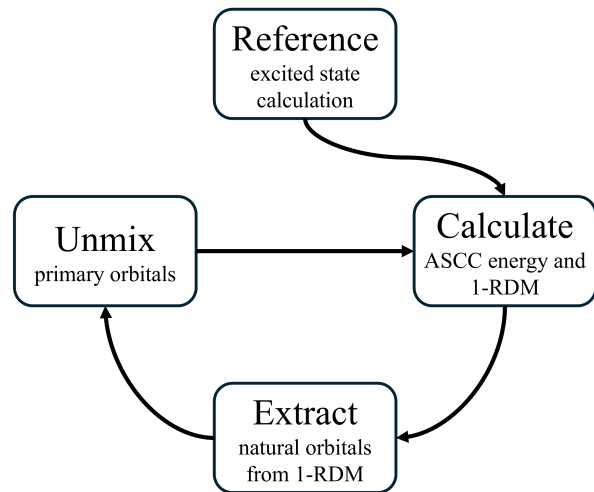


Figure 2. Schematic of the natural orbital refinement procedure. See Section II C for details.

more closely mirrors the ground state, with the only difference being the off-diagonal all primary blocks being complete through the higher third order too. Interestingly, when including partial linearization, the perturbative completeness of the 1-RDM is equivalent for all three implementations due to the missing nonlinear \hat{T} contributions. Furthermore, they are less accurate than ASCC^(M,1). Based off this fact alone, it seems an unnecessary expense to include any higher order contributions when performing partial linearization. Indeed, we will see in Section III D that, when using partial linearization, including the extra amplitudes is not helpful.

C. Natural Orbital Refinement

In single-CSF ASCC, the dependence of the ansatz on the reference wave function comes through the starting molecular orbitals and the designation of which are the hole and particle orbitals. As different reference methods (CIS, TD-DFT, ESMF, etc.) provide different orbital shapes, ASCC's results are expected to vary at least slightly from one reference to another. Ideally, the reference orbitals would be determined by the higher accuracy ASCC method as opposed to the often more affordable (and less accurate) reference methods. With the ability to evaluate the 1-RDM and thus ASCC's natural orbitals (NOs), a straightforward (if a bit crude) way to explore this concept is to iteratively feed the NOs outputted by one ASCC calculation in as the starting molecular orbitals for another, as depicted in Figure 2. In other words, this approach allows ASCC to refine its own orbitals, potentially eliminating any differences that might have arose from starting with CIS vs TD-DFT vs ESMF, assuming that this SCF-like iteration converges towards the same fixed point starting from each of those unique references.

While this procedure sounds straightforward, an interesting problem arises very quickly. Tuckman et al. have previously noted that ASCC is prone to symmetry violations from a “downward ladder effect” caused from the new zeroth order Hamiltonian being able to de-excite in the primary subspace.²³ Because of this symmetry violation, the off diagonal elements of the 1-RDM between orbitals of different symmetry representations do not necessarily have to be zero, meaning that, upon diagonalization, mixing between orbitals of different symmetries can occur. As the hole and particle orbitals are typically close to half-filled in an excited state, their diagonal elements in the 1-RDM are nearly equal, and so even small symmetry violations in their off-diagonal elements can result in significant particle-hole mixing in the NOs, regardless of whether such mixing is symmetry forbidden. To minimize this effect, we project the original particle and hole orbitals into the two-dimensional subspace of the new hole and particle NOs to form near-natural hole and particle orbitals that are much more resilient to symmetry breaking. Note that the same issue does not arise for other orbitals, as the 1-RDM diagonal entries for occupied, hole, particle, and unoccupied orbitals are roughly 2.0, 1.0, 1.0, and 0.0, respectively, making the particle-hole case the only near-degeneracy case that matters (ASCC is invariant to mixings between doubly occupied orbitals and mixings between unoccupied orbitals).

D. Population Analysis and Dipole Moments

In order to approximate the electronic change in populations from the ground to the excited state, both a Mulliken and a Löwdin population analysis were employed. These analyses are two of the most common population schemes utilized due to their simplistic form and long-standing history.¹¹⁴ The charge on a given atom A is

$$q_A = Z_A - \sum_{\nu \in A} (\gamma_{AO} S)_{\nu\nu} \quad (17)$$

for a Mulliken-style analysis and

$$q_A = Z_A - \sum_{\nu \in A} (S^{1/2} \gamma_{AO} S^{1/2})_{\nu\nu} \quad (18)$$

for a Löwdin-style analysis, where Z_A is the nuclear charge of atom A , ν are the atomic orbitals located on atom A , γ_{AO} is the 1-RDM in the atomic orbital (AO) basis, and S is the atomic overlap matrix.^{82,115} The difference between the excited state and ground state atomic populations were taken to focus specifically on the charge transfer occurring. These changes were then summed over within specific moieties to gather the electronic change of an entire group instead of a specific atom. While both the Mulliken and Löwdin population analyses are known to depend on the chosen basis set and therefore can be misleading to trust in absolutes,^{116,117}

we attempt to mitigate these uncertainties by focusing specifically on changes between the ground and excited charges, overall charges of entire fragments instead of individual atoms, and on a more qualitative analysis. Furthermore, by comparing both population schemes against each other, we lessen the chance that our results are simply a product of fortune from one specific scheme.

For excited state dipole moments, the 1-RDM in the AO basis is also needed. However, as mentioned previously, for completely accurate dipole moment calculations the response of the molecular orbitals to the changing electric field is required. These were neglected as we opted for an orbital unrelaxed 1-RDM in this study. After converting the 1-RDM into the AO basis, tracing the product of it and the atomic orbital’s response to the electric field yields the electronic dipole, which can be added to the nuclear dipole for the total dipole.

III. RESULTS

A. Computational Details

Following the study by Quady et al., CIS,¹¹⁸ EOM-CCSD,⁴⁻⁶ TD-DFT,¹⁻³ and ESMF⁴⁹⁻⁵¹ were all used as excited state references in both the natural orbital refinement and dipole moment calculations.⁷⁸ For more details on the specifics of how initial guesses were generated from the references, we refer the reader to their paper. For the population analysis tests, ESMF was used as a reference in all systems except for the tetrafluoroethylene-ethylene charge transfer, where instead CIS was used as a reference due to convergence issues with the ESMF solution. CIS calculations were conducted with PySCF¹¹⁹ while both EOM-CCSD and TD-DFT/ ω B97X-V¹²⁰ calculations were performed with Q-Chem 6.2.¹²¹ None of the calculations used the frozen core approximation, though comparisons to references that did utilize the frozen core approximation are still performed; the difference between utilizing this approximation and not is very small (~ 0.02 eV), so these comparisons are still valid to make.^{122,123} Q-Chem’s excited state analysis module was used to calculate the transition density matrices and natural orbitals necessary for creating (PL)ASCC’s starting guess, along with the excited state dipole moments.¹²⁴⁻¹²⁸ The calculation of orbital unrelaxed and relaxed LR-CCSD excited state dipoles was performed in MRCC.¹²⁹⁻¹³³ Orbital visualizations were performed using Gabedit.¹³⁴ The molecular structures used for the valence and Rydberg excitation systems of the natural orbital refinement and the dipole moment calculations can be found in the supporting information of the respective QUEST benchmark studies.^{122,123} The geometries for the charge transfer systems can be found in the supporting information of Kuzma et al.¹³⁵ and Tuckman et al.²³ The geometries for the water flyby test system explored using population analyses were taken from Clune et al.⁵⁷ For totally symmetric excitations where (PL)ASCC demonstrates two

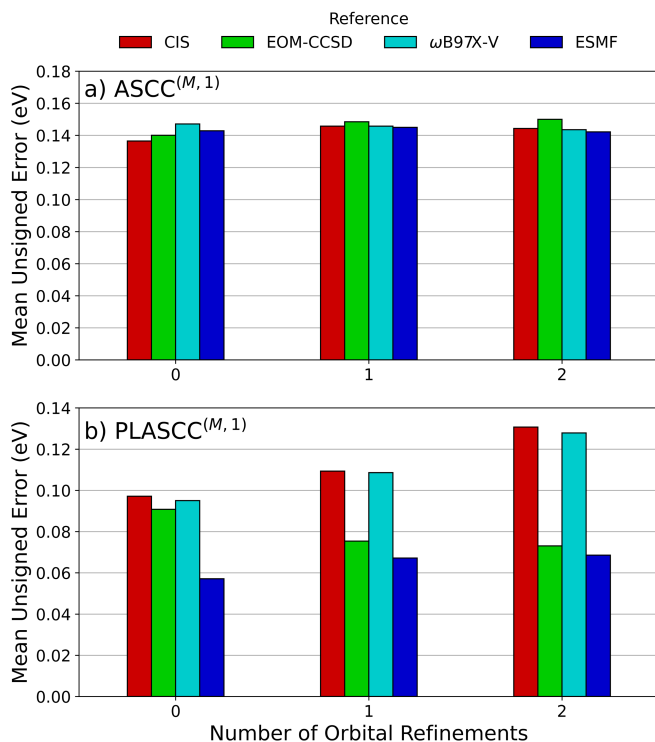


Figure 3. The mean unsigned excitation errors of 14 valence and Rydberg states from 5 molecules when starting from CIS, TD-DFT, EOM-CCSD, or ESMF starting points for a) ASCC^(M,1) and b) PLASCC^(M,1) after 0, 1, or 2 natural orbital refinements.

unique solutions,²³ we still average the two together to get one final energy or dipole moment value.

B. ASCC Orbital Refinement

Utilizing the framework outlined in Section II C, we first explored ASCC natural orbital refinement on some simple valence and Rydberg excitations previously examined by Quady et al.⁷⁸ Specifically, 14 states coming from 5 different molecules were examined, with vertical excitation energy comparisons to high level theory from the QUEST database.^{122,123} CIS, EOM-CCSD, TD-DFT/ ω B97X-V, and ESMF were all used as references for both ASCC^(M,1) and PLASCC^(M,1). The natural orbital refinement procedure was carried out for two iterations on each state, resulting in three (PL)ASCC^(M,1) energies for each reference: without orbital refinement, with 1 orbital refinement, and with 2 orbital refinements. The precise energy values from each calculation can be found in the Supporting Information.

As seen in Figure 3, performing the natural orbital refinements seemed to have little effect on the overall accuracy of the vertical excitation energies in ASCC^(M,1). However, these refinements did reduce the methods’ dependence on the starting point, as seen in Figure 4. In

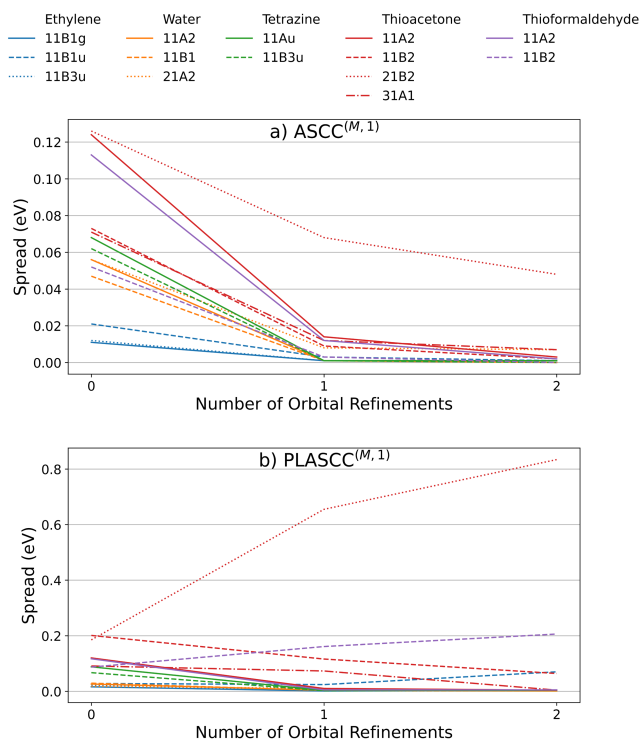


Figure 4. The spread in the excitation energies when starting from CIS, TD-DFT, ESMF, or EOM-CCSD starting points for a) ASCC^(M,1) and b) PLASCC^(M,1) after 0, 1, or 2 natural orbital refinements. The spread is measured as the difference between the maximum and minimum excitation energy predictions.

all but one state, two iterations of natural orbital refinement brought all the starting points’ ASCC energies to within 0.01 eV of each other. In that one state (the 2^1B_2 transition in thioacetone), the refinements are mitigating the starting point dependence, but more slowly, with a roughly 0.05 eV spread left after two cycles of refinement. We also note that in the totally symmetric states, we witness convergence towards two unique solutions, indicating that each of the two ansätze is converging towards separate orbital fixed points. With only two such states in this test set, though, we make no conclusions about whether one or the other ansatz is more accurate.

While PLASCC^(M,1) typically demonstrates a lower error in vertical excitations, it did not seem to behave as well under orbital refinement as ASCC^(M,1) did. In fact, for 3 of the 14 states, the standard deviation of the 4 references grew after performing natural orbital refinements, as seen in Figure 4, indicating potential divergence between the various references instead of the desired convergence. This might be caused in part by the slightly less accurate 1-RDM discussed in Section II B, but as only the occupied/virtual block was of a different order, we cannot conclude that it is guaranteed to be solely from this perturbative difference. On the other hand, convergence to within 0.01 eV after two orbital re-

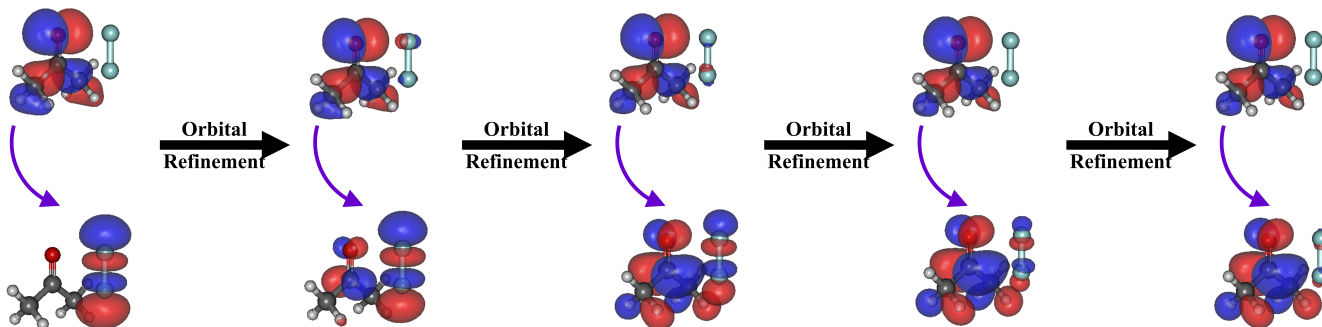


Figure 5. The hole and particle orbitals demonstrating symmetry contamination for the acetone-difluorine charge transfer system throughout the natural orbital refinement procedure. The original reference was ESMF and $\text{ASCC}^{(M,1)}$ was utilized to perform the orbital refinements.

refinements was still observed for 10 of the 14 states. Additionally, the 1^1B_2 state of thioacetone showed signs of converging to this tight threshold more slowly, with an original energetic discrepancy between references of 0.20 eV shrinking to only 0.06 eV. Interestingly, the initial reference seemed to be much more significant for PLASCC. In the 3 states where divergence was observed, it seemed to be the case that EOM-CCSD and ESMF were converging towards one solution and CIS and $\omega\text{B97X-V}$ converging towards another.

After seeing success for reaching a stationary point for all of the $\text{ASCC}^{(M,1)}$ calculations on simpler systems, we decided to test the more complex charge transfer (CT) systems that ASCC typically performs quite well at.²³ Predicting that these more difficult systems would be tougher to converge, we performed the NO refinement procedure for four iterations for each state, resulting in five (PL)ASCC^(M,1) energies for each reference. While at times we did witness convergence to a single ASCC reference-independent solution with an error comparative to that of the original references, we also noticed issues appearing from the amplification of symmetry breaking. As stated before, we were manually attempting to unmix the new hole and particle orbitals by projecting them into the subspace of the reference hole and particle, but if the symmetry breaks a bit more each iteration, more and more of the Aufbau coefficient starts appearing when it should be 0. This resulted in some states whose references converged together, but to an incorrect solution that is not physically possible. An example of convergence to a different solution with significant symmetry contamination is depicted in Figure 5. Unfortunately, this wasn’t always visible with just 1 or 2 orbital refinements, sometimes requiring 3 or 4 before any significant energetic issues arose. Once these problems did appear, we often then had difficulty converging the remaining calculations, indicative of the poor, symmetry contaminated starting points provided from the previous orbital refinements (see Supporting Information for calculation diagnostics). Of the 7 total CT states tested, $\text{ASCC}^{(M,1)}$

converged to a stationary point on only 3, those being the ammonia-difluorine 2^1A_1 , the pyrazine-difluorine 2^1A_2 , and the ammonia-oxygendifluorine $4^1A'$. The remaining 4 states all experienced symmetry contamination in at least 2 of the 4 references tested, and with new starting points based on these poor results, the calculations yielded nonphysical solutions if the energetic convergence threshold was even reached.

$\text{PLASCC}^{(M,1)}$ performed quite similarly on the CT systems, with the only states truly reaching convergence being ammonia-difluorine’s 2^1A_1 and tetrafluoroethylene-ethylene’s 5^1B_1 . Acetone-difluorine’s $3^1A''$ also seemed to reach a stationary point when using EOM-CCSD or ESMF as a reference, but not when using CIS or TD-DFT, again hinting at a potentially stronger reference dependence for $\text{PLASCC}^{(M,1)}$ than $\text{ASCC}^{(M,1)}$ for response properties. Unfortunately, the other 5 tests all either failed to converge or reached nonphysical solutions. Overall, these results demonstrate that stationary points still have the potential to be achieved, even when using the poorer 1-RDM only complete through first order and without the utilization of an acceleration scheme to improve convergence. However, this is currently only true for smaller systems where the symmetry violations are much less pronounced. To explore whether stationarity could still be achieved for larger systems, more careful consideration of how to reduce the problems arising from symmetry violations is needed.

C. Population Analysis

Despite the mixed results when attempting natural orbital refinement on the charge transfer states, the excitation energies predicted by plain $\text{ASCC}^{(M,1)}$ for these states are more accurate than those predicted by EOM-CCSD.²³ This observation begs the question: to what degree do these methods agree or disagree about how much charge is being transferred during these excitations? To evaluate this, we have carried out both Mul-

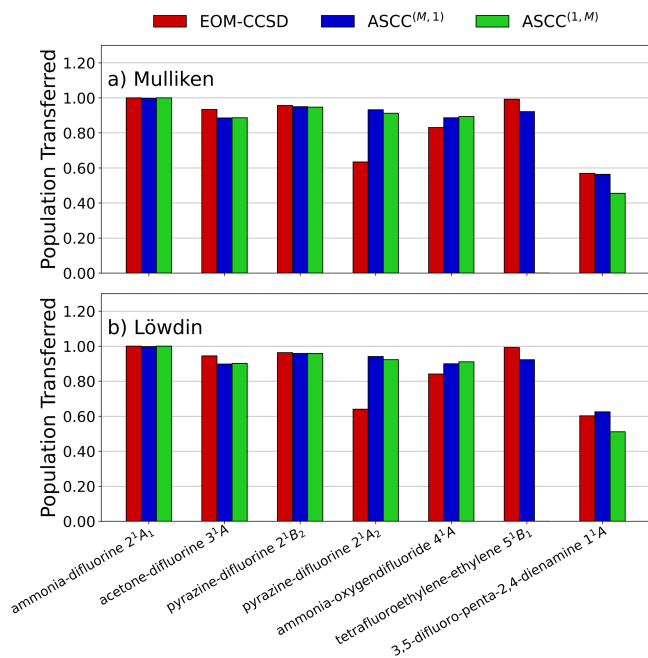


Figure 6. The a) Mulliken and b) Löwdin populations transferred from the charge transfer excitations for both EOM-CCSD and ASCC.

liken and Löwdin population analyses. For the intermolecular charge transfers, we add together the populations of the atoms in the donor molecule and look at how this total changes between the ground and excited state. For the 3,5-difluoro-penta-2,4-dienamine intramolecular charge transfer, we take a similar approach, with the donor moiety defined as the primary amine and its neighboring CH₂ group.

As shown in Figure 6, EOM-CCSD and ASCC agree about how much charge gets transferred to within 0.1 electrons of each other for six of the seven systems tested. We also see that the Mulliken population results are closely matched by those of the Löwdin approach. The largest disagreement between EOM-CCSD and ASCC is seen in the pyrazine-difluorine 2¹A₁ state, where ASCC predicts that almost a whole electron transfers, while EOM-CCSD predicts that only a little more than 0.6 electrons transfer. Given that this is an intermolecular charge transfer, we would expect roughly a whole electron to transfer (although note that this would not be our expectation for the right-most case in the figure, as that system contains an intramolecular CT).

Without higher-level results to compare to (none of the codes we have access to can evaluate populations for CC3 excited states), it is difficult to draw firm conclusions about whether disagreements between EOM-CCSD and ASCC in Figure 6 imply higher accuracy for one method or the other. Intuition suggests that ASCC offers some advantage in the pyrazine-difluorine 2¹A₁ state, but overall the good agreement in the other tests leaves us with the primary conclusion that EOM-CCSD and ASCC tend

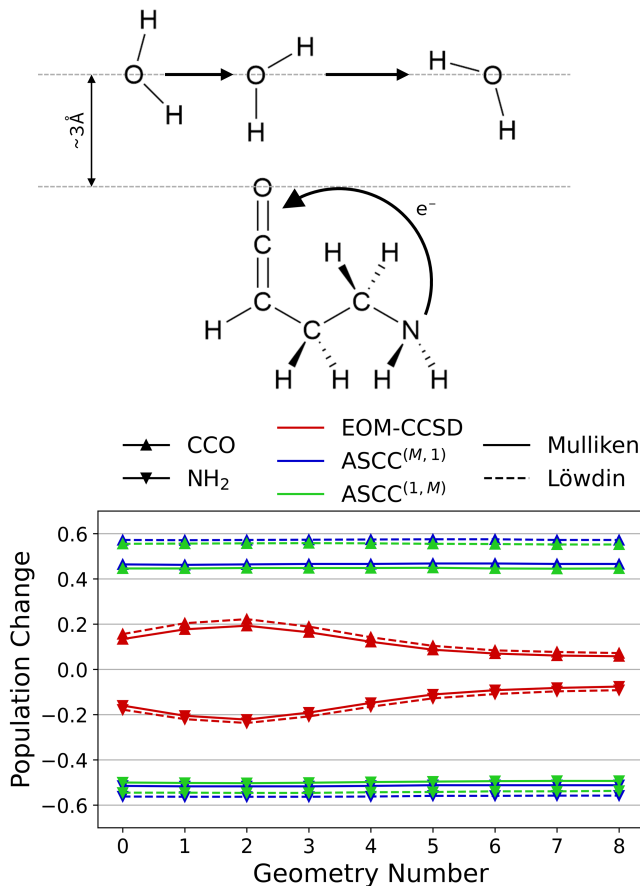


Figure 7. A schematic of the water flyby test system is shown above the EOM-CCSD and ASCC population changes of the CCO and NH₂ moieties upon excitation to the ¹A' CT state.

to agree with each other on populations in CT states.

Previous work has, however, made us aware of an intramolecular CT example in which ASCC produces a qualitatively more correct excited state than EOM-CCSD, and so it is also worth considering their population predictions in that case. Specifically, this test involves moving a water molecule past a donor-bridge-acceptor molecule with an intramolecular charge transfer from the nitrogen lone pair to the in-plane π* orbital on the ketene moiety (the ¹A' charge transfer state), shown in Figure 7. Previously, it was shown that EOM-CCSD incorrectly mixes the CT state with a low-lying Rydberg excitation in a roughly 50:50 ratio.^{24,57} This implies that it should demonstrate less explicit charge transfer character, especially if any of the AOs on the primary amine contribute to the disperse MO of the Rydberg state. Additionally, interactions between the moving water molecule and the large MOs of the Rydberg excitation would alter the amount of population transfer occurring, which wouldn't be as dramatic if only the n → π* charge transfer was involved. Indeed, these are both exactly

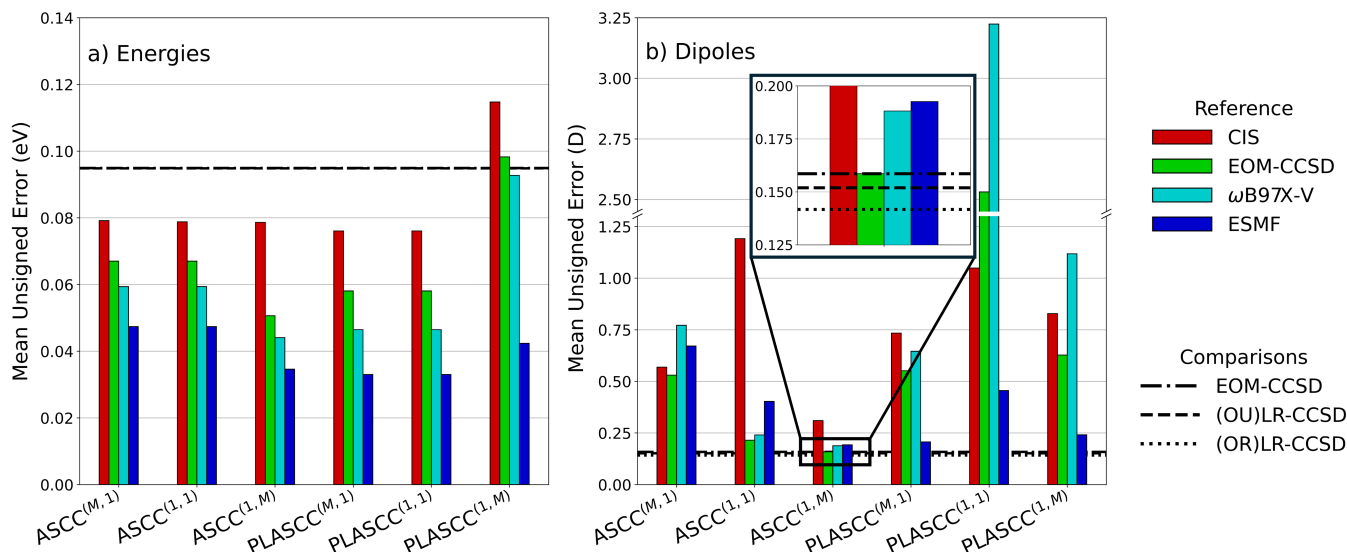


Figure 8. The mean unsigned errors for the a) vertical excitation energy (eV) and b) excited state dipole moments (D) of the various ASCC-based methods with references of CIS, EOM-CCSD, ω B97X-V, and ESMF. The black lines show comparisons to EOM-CCSD, (OU)LR-CCSD, and (OR)LR-CCSD, which all produce the same energies.

what we see in Figure 7. The ketene moiety where the π^* bond is localized gains a constant electronic population of roughly 0.5 electrons as the water passes by for both ASCC^(M,1) and ASCC^(1,M), but EOM-CCSD predicts varying transfers ranging from 0.05 to 0.25 electrons, depending on the water’s position. Similarly, the change on the amine group remains constant for ASCC at around -0.5 , whereas for EOM-CCSD it again fluctuates when the water is moved. This example demonstrates that ASCC’s ability to correctly place the CT excitation below the Rydberg states and thus avoid CT/Rydberg mixing is very significant for its population predictions, especially when compared to the predictions of EOM-CCSD.

D. Dipole Moments

Excited state dipole moment calculations were performed on 14 states across 5 different molecules. As before, CIS, EOM-CCSD, TD-DFT/ ω B97X-V, and ESMF were all used as references for all 3 variations of ASCC and PLASCC discussed in Section II B. The overall dipole moments are compared to calculations performed by Chrayteh et al. at the LR-CCSDTQP level of theory for H₂O, CO, and H₂S and the LR-CCSDTQ level of theory for formaldehyde and thioformaldehyde.⁹⁴ These high level LR-CC calculations all included orbital relaxation from coupled-perturbed Hartree Fock, but, as discussed previously, this effect is mitigated as more excitations are included, so it is still valid to compare to our unrelaxed ASCC values. We have also included comparisons to EOM-CCSD, orbital unrelaxed (OU) LR-CCSD, and orbital relaxed (OR) LR-CCSD to demonstrate the mag-

nitude of errors common in these types of calculations. The results can be seen in Figure 8.

As expected, every variant of ASCC and nearly every variant of PLASCC performs slightly better than EOM-CCSD in terms of vertical excitation energies for the systems examined. As altering the number of left-hand amplitudes by itself has no effect on the energies, (PL)ASCC^(M,1) and (PL)ASCC^(1,1) both give the same results. When increasing the number of right-hand amplitudes for ASCC, the energies improve, which is rather unsurprising as the energy becomes correct through third order instead of second order. On the other hand, it seems that the addition of more amplitudes to PLASCC has the opposite effect, actually becoming worse with additional \hat{T} amplitudes. This isn’t especially surprising, as the inclusion of these additional amplitudes offsets the original design to balance their missing contributions. Thus, an update to this partial linearization trick is required to have the same intended effects of balancing further missing contributions. For this small subset of tests, ASCC with the additional \hat{T} amplitudes seemed to perform roughly equal to PLASCC without them, but more testing should be conducted before concluding that this is typically observed.

Upon investigation of dipole moments, the accuracy of the results depended heavily upon the method of use. For ASCC, we see the systematic improvability expected from the perturbative correctness of the various 1-RDMs. While the GS cost-equivalent ASCC^(M,1) performed quite poorly, maintaining perturbative equivalence to other methods with ASCC^(1,M) yielded errors on par with these other methods. While this test set is still quite limited, this begs the question of whether ASCC would outperform these other methods where it

usually outperforms them for energies by a more significant margin, such as charge-transfer systems. Additionally, it would be interesting to explore how significantly the addition of orbital relaxation reduces the effects of the reference itself.

Unfortunately, this same story is not true for PLASCC. As one might have expected based solely from the fact that adding in additional amplitudes does not actually improve the 1-RDM perturbative correctness for PLASCC, adding in more amplitudes also did not improve the accuracy of the dipole moments. In fact, it often actually decreased the accuracy of the calculations, pointing again quite strongly to a more careful consideration of how to perform partial linearization for both more amplitudes and for canceling potential errors on the left-hand side. Additionally, PLASCC again demonstrated a much larger dependence upon the original reference chosen for dipole moments, with ESMF references performing better than others by at least a quarter of a Debye, and often more, irrespective of the perturbative truncation scheme employed.

IV. CONCLUSION

We have derived the excited state one-body reduced density matrix for single-CSF Aufbau suppressed coupled cluster theory for the evaluation of one-body properties. The 1-RDM was first used to calculate natural orbitals in an attempt to find a reference-independent stationary point for ASCC. For simple valence and Rydberg systems, we showed that this can be achieved, but the converged solution was not significantly more accurate than any of the solutions using the original references. However, with more difficult systems like charge transfer excitations, convergence was reached on only a fraction of the tests, indicating that a closer analysis of the effects and potential prevention of symmetry violation in both the right- and left-hand amplitudes should occur. For this reason, we currently do not recommend performing natural orbital refinement within ASCC as a general strategy, but we have hope that an improved approach to reach the reference-independent stationary point can be devised. Despite this setback, we still showed that ASCC's response can be useful where other methods struggle; this was demonstrated through the successful predictions of minimal change to atomic populations on a charge transfer despite a small modification to the surroundings, whereas EOM-CCSD incorrectly predicted less charge transfer characteristics and a larger dependence upon the surroundings. Through a perturbative analysis, we found that when only including the first order excitation amplitudes (similar to ground state CCSD), the 1-RDM is significantly less accurate than its ground state counterpart. However, upon the inclusion of some additional amplitudes that don't change the asymptotic scaling, we can complete the 1-RDM through the same orders of PT as CCSD. While doing so had minimal effect on the

accuracy of vertical excitation energies, for which regular ASCC already performed well in the systems tested, the response-informed variant ASCC^(1,M) demonstrated a significantly higher accuracy in predicting excited state dipole moments, roughly on par with orbital unrelaxed LR-CCSD. Thus, while ASCC^(1,M) mostly reproduces the accuracy of EOM-CCSD for excited state populations and dipoles, it should be emphasized that it does so while simultaneously delivering improved excitation energies in CT systems.

The completion of analytic first derivatives would allow for multiple new areas to explore in the future. Likely one of the most exciting next steps is the addition of the 2-RDM in order to calculate nuclear gradients, which can in turn be used for excited state geometry optimizations. To be completely accurate, one would also want to include the response of the initial reference's orbital basis so that orbital relaxations from the perturbation can be taken into account, which are especially important when nuclei are moved. Additionally, if one had the response of the reference method, we could extend the results past the 1-CSF case, allowing for the calculation of properties even if the state is multireference in character. With analytic first derivatives completed, a reformulation of PLASCC, or devising an alternative to PLASCC, to better accommodate response accuracy should also be explored. Focusing instead on speed, one could extend the Lagrangian formalism to calculate properties of the excited state using a second-order Aufbau suppressed perturbation theory, which is non-iterative $O(N^5)$ scaling, as originally proposed by Tuckman and Neuscamman.²⁴ This would also mitigate the effect of adding in the additional amplitudes required to bring ASCC's response accuracy on par with that of the ground state. Combining these approaches, one could also potentially nest the CC response equations within the perturbation code, providing CC level accuracy at the PT level of cost.

V. APPENDIX

A. Perturbative Analysis of the Response Amplitudes and 1-RDM

While the Lagrange formalism is a useful way to represent the ASCC equations concisely, it can alternatively be useful to work within the framework of fully connected diagrams, in which the residual equations for the lambda amplitudes become

$$0 = \langle \phi_0 | (1 + \hat{\Lambda}) \left((e^{\hat{S}^\dagger} \hat{H}_N)_C e^{\hat{T}} \right)_C | \phi_{ij\dots}^{ab\dots} \rangle_C + \sum_{\substack{k < l < \dots \\ c < d < \dots}} \langle \phi_0 | (e^{\hat{S}^\dagger} \hat{H}_N)_C e^{\hat{T}} | \phi_{kl\dots}^{cd\dots} \rangle_C \langle \phi_{kl\dots}^{cd\dots} | \hat{\Lambda} | \phi_{ij\dots}^{ab\dots} \rangle_C \quad (19)$$

with \hat{H}_N representing the normal ordered Hamiltonian and the subscript C designating only fully connected

diagrams.^{92,93} This representation will allow us to specify which term specifically leads to the odd behavior observed in the following perturbative analysis. However, for uncovering the zeroth order $\hat{\Lambda}$ amplitudes, it is arguably simpler to focus on just the wavefunction itself. As discussed in Section II A and demonstrated by Tuckman et al.,²³ evaluating the Taylor series expansion of Equation (1) at zeroth order using definitions from Equations (12) and (13) leads to the result that the zeroth order wavefunction is simply $\hat{S}_{1\text{-CSF}}|\phi_0\rangle$. From here on out, we will drop the 1-CSF label, as this analysis is confined to this specific type of system. As we similarly desire the zeroth order bra to be $\langle\phi_0|\hat{S}^\dagger$, then we must ensure that the left projection onto our Hamiltonian in the Lagrangian simplifies to this, providing an expression relating $\hat{\Lambda}^{(0)}$ to the zeroth order wavefunction.

$$\langle\phi_0|\hat{S}^\dagger = \langle\phi_0|\left(1 + \hat{\Lambda}^{(0)}\right) e^{-\hat{T}^{(0)}} e^{\hat{S}^\dagger} \quad (20)$$

$$= \langle\phi_0|\left(1 + \hat{\Lambda}^{(0)}\right) e^{-\hat{S} + \frac{1}{2}\hat{S}^2} e^{\hat{S}^\dagger} \quad (21)$$

$$= \langle\phi_0|\left(1 + \hat{\Lambda}^{(0)}\right) \left(1 - \hat{S} + \hat{S}^2\right) \left(1 + \hat{S}^\dagger + \frac{1}{2}(\hat{S}^\dagger)^2\right) \quad (22)$$

From Equation (22), we find that $\hat{\Lambda}^{(0)}$ must reside solely within the primary subspace just like $\hat{T}^{(0)}$, as any extension outside of this subspace could not be balanced using just \hat{S} and its adjoint. Equivalently, this implies that $\hat{\Lambda}^{(0)} = a\hat{S}^\dagger + b(\hat{S}^\dagger)^2$. By right projecting with $|\phi_0\rangle$ and $\hat{S}^2|\phi_0\rangle$ onto both sides of Equation (22), we get a two-by-two system of equations. Solving this, we find that $a = b + 1$ from the first equation and $a = -(b + 1)$ in the second, implying that $a = 0$ and that $b = -1$. Thus, we are left with the result from Equation (16), that $\hat{\Lambda}^{(0)} = -(\hat{S}^\dagger)^2$. A perturbative analysis to zeroth order of Equation (19) yields an equivalent result, further confirming that this Taylor series approach is valid.

With this definition of $\hat{\Lambda}^{(0)}$ and Equation (19), one can verify that the additional slices of the triples and quadruples discussed in Section II B are indeed nonzero at first order. To demonstrate this, we will show that there is a nonzero contribution to the slice of quadruples at first order, as this term is the most unusual. By working in the untruncated limit, consider the right projection with the slice of the quadruples containing four primary indices in Equation (19). To first order, the first term only provides nonzero contributions containing $\hat{\Lambda}_4^{(1)}$ itself. If the second term were zero, like in the ground state, then this would guarantee $\hat{\Lambda}_4^{(1)} = 0$. However, the second term can provide contribution from the product of the double de-excitation of $\hat{H}^{(1)}$ in the solely non-primary space and the double de-excitation of $\hat{\Lambda}^{(0)}$ in the all primary space. While this term alone is enough to demonstrate that the quadruples are not all zero, there is an additional contribution from the single primary de-excitation resulting from the similarity transformation of $\hat{H}^{(0)}$ with \hat{S}^\dagger paired with the first order $\hat{\Lambda}_3^{(1)}$ with two primary indices and a

primary de-excitation. These contributions arise solely due to the $\hat{\Lambda}$ amplitudes containing contributions from disconnected terms, which is unlike the \hat{T} amplitudes.

Completing a full perturbative analysis of both the \hat{T} and $\hat{\Lambda}$ operators at each order, it is likely unsurprising that more differences appear at higher orders. We will focus our attention on $\text{ASCC}^{(M,1)}$, where we can show that these differences lead to the asymmetric perturbative accuracy of the 1-RDM shown in Figure 1. All of the \hat{T} amplitudes that are included in $\text{ASCC}^{(M,1)}$ are complete through second order, but there are no pieces complete through third order. On the other hand, since $\hat{\Lambda}$ is missing some parts of its first order amplitudes, the only amplitudes complete through second order are restricted to the all primary singles and doubles and the all non-primary singles. For example, the mixed single de-excitation of $\hat{\Lambda}_1^{(2)}$ has contribution from the missing $\hat{\Lambda}_3^{(1)}$ slice with two primary indices and one primary de-excitation when contracted with the slice of $\hat{T}_3^{(1)}$ with three primary indices and one primary excitation, demonstrated by the diagrammatic sketch of Equation (23). Here, the thick black bar on top designates $\hat{\Lambda}$, whereas the thinner black bar on top designates \hat{S}^\dagger .

With this in mind, consider the γ_{ih} and γ_{hi} elements of the 1-RDM. For γ_{ih} , the non-primary creation operator must be balanced by a \hat{T} operator, implying that \hat{T} must be at least first order, restricting $\hat{\Lambda}$ to first or zeroth order. This does not cause any issues, as we have all $\hat{T}^{(1)}$ and the corresponding $\hat{\Lambda}^{(1)}$ needed to balance them out. Alternatively, if we wanted to use a $\hat{T}^{(2)}$, then we are restricted to $\hat{\Lambda}^{(0)}$, forcing us to use a slice of $\hat{T}_2^{(2)}$ with three primary indices, which we also have. Thus, γ_{ih} is complete through second order. However, for γ_{hi} , these restrictions are reversed. Thus, a valid term appears containing the all-primary single excitation of $\hat{T}_1^{(0)}$ and the mixed single de-excitation of $\hat{\Lambda}_1^{(2)}$, of which we don't have because of contributions like those in Equation (23). This type of interaction leads to the imbalances of the perturbative accuracy in the 1-RDM witnessed in Figure 1. Similarly, one can show that the removal of terms from the partial linearization of PLASCC will reduce which parts of \hat{T} and $\hat{\Lambda}$ are complete through second order and higher, resulting in the lower perturbative accuracy of PLASCC in these same types of situations.

VI. ACKNOWLEDGEMENTS

This work was supported by the National Science Foundation, Award Number 2320936. Calculations were performed using the Savio computational cluster resource provided by the Berkeley Research Computing program

at the University of California, Berkeley. C.B. acknowledges that this material is based upon work supported by the U.S. Department of Energy, Office of Science, Office of Advanced Scientific Computing Research, Department of Energy Computational Science Graduate Fellowship under Award Number DE-SC0025528. H.T. acknowledges that this material is based upon work supported by the National Science Foundation Graduate Research Fellowship Program under Grant No. DGE 2146752. Any opinions, findings, and conclusions or recommendations expressed in this material are those of the authors and do not necessarily reflect the views of the Department of Energy or the National Science Foundation.

VII. REFERENCES

- ¹Runge, E.; Gross, E. K. U. Density-Functional Theory for Time-Dependent Systems. *Phys. Rev. Lett.* **1984**, *52*, 997–1000.
- ²Burke, K.; Werschnik, J.; Gross, E. K. U. Time-Dependent Density Functional Theory: Past, Present, and Future. *J. Chem. Phys.* **2005**, *123*, 062206.
- ³Casida, M. E.; Huix-Rotllant, M. Progress in Time-Dependent Density-Functional Theory. *Annu. Rev. Phys. Chem.* **2012**, *63*, 287–323.
- ⁴Rowe, D. J. Equations-of-Motion Method and the Extended Shell Model. *Rev. Mod. Phys.* **1968**, *40*, 153–166.
- ⁵Stanton, J. F.; Bartlett, R. J. The Equation of Motion Coupled-Cluster Method. A Systematic Biorthogonal Approach to Molecular Excitation Energies, Transition Probabilities, and Excited State Properties. *J. Chem. Phys.* **1993**, *98*, 7029–7039.
- ⁶Krylov, A. I. Equation-of-Motion Coupled-Cluster Methods for Open-Shell and Electronically Excited Species: The Hitchhiker’s Guide to Fock Space. *Annu. Rev. Phys. Chem.* **2008**, *59*, 433–462.
- ⁷Loos, P.-F.; Comin, M.; Blase, X.; Jacquemin, D. Reference Energies for Intramolecular Charge-Transfer Excitations. *J. Chem. Theory Comput.* **2021**, *17*, 3666–3686.
- ⁸Knysh, I.; Lipparini, F.; Blondel, A.; Duchemin, I.; Blase, X.; Loos, P.-F.; Jacquemin, D. Reference CC3 Excitation Energies for Organic Chromophores: Benchmarking TD-DFT, BSE/GW, and Wave Function Methods. *J. Chem. Theory Comput.* **2024**, *20*, 8152–8174.
- ⁹Širůček, J.; Le Guennic, B.; Damour, Y.; Loos, P.-F.; Jacquemin, D. Excited-State Absorption: Reference Oscillator Strengths, Wave Function, and TDDFT Benchmarks. *J. Chem. Theory Comput.* **2025**, *21*, 4688–4703.
- ¹⁰Wang, J.; Durbeej, B. How Accurate Are TD-DFT Excited-State Geometries Compared to DFT Ground-State Geometries? *J. Comput. Chem.* **2020**, *41*, 1718–1729.
- ¹¹González, L.; Escudero, D.; Serrano-Andrés, L. Progress and Challenges in the Calculation of Electronic Excited States. *ChemPhysChem* **2012**, *13*, 28–51.
- ¹²Shao, Y.; Head-Gordon, M.; Krylov, A. I. The Spin-Flip Approach within Time-Dependent Density Functional Theory: Theory and Applications to Diradicals. *J. Chem. Phys.* **2003**, *118*, 4807–4818.
- ¹³Bernard, Y. A.; Shao, Y.; Krylov, A. I. General Formulation of Spin-Flip Time-Dependent Density Functional Theory Using Non-Collinear Kernels: Theory, Implementation, and Benchmarks. *J. Chem. Phys.* **2012**, *136*, 204103.
- ¹⁴Krylov, A. I. Size-Consistent Wave Functions for Bond-Breaking: The Equation-of-Motion Spin-Flip Model.
- ¹⁵Krylov, A. I. Spin-Flip Equation-of-Motion Coupled-Cluster Electronic Structure Method for a Description of Excited States, Bond Breaking, Diradicals, and Triradicals. *Acc. Chem. Res.* **2006**, *39*, 83–91.
- ¹⁶Nooijen, M.; Bartlett, R. J. Similarity Transformed Equation-of-Motion Coupled-Cluster Theory: Details, Examples, and Comparisons. *J. Chem. Phys.* **1997**, *107*, 6812–6830.
- ¹⁷Bartlett, R. J. The Coupled-Cluster Revolution. *Mol. Phys.* **2010**, *108*, 2905–2920.
- ¹⁸Musiał, M.; Perera, A.; Bartlett, R. J. Multireference Coupled-Cluster Theory: The Easy Way. *J. Chem. Phys.* **2011**, *134*, 114108.
- ¹⁹Kuś, T.; Krylov, A. I. Using the Charge-Stabilization Technique in the Double Ionization Potential Equation-of-Motion Calculations with Dianion References. *J. Chem. Phys.* **2011**, *135*, 084109.
- ²⁰Kuś, T.; Krylov, A. I. De-Perturbative Corrections for Charge-Stabilized Double Ionization Potential Equation-of-Motion Coupled-Cluster Method. *J. Chem. Phys.* **2012**, *136*, 244109.
- ²¹Perera, A.; Molt, R. W.; Lotrich, V. F.; Bartlett, R. J. Singlet-Triplet Separations of Di-Radicals Treated by the DEA/DIP-EOM-CCSD Methods. *Theor Chem Acc* **2014**, *133*, 1514.
- ²²Tuckman, H.; Neuscammann, E. Aufbau Suppressed Coupled Cluster Theory for Electronically Excited States. *J. Chem. Theory Comput.* **2024**, *20*, 2761–2773.
- ²³Tuckman, H.; Ma, Z.; Neuscammann, E. Improving Aufbau Suppressed Coupled Cluster through Perturbative Analysis. *J. Chem. Theory Comput.* **2025**, *21*, 3993–4005.
- ²⁴Tuckman, H.; Neuscammann, E. Fast and Accurate Charge Transfer Excitations via Nested Aufbau Suppressed Coupled Cluster. *J. Phys. Chem. Lett.* **2025**, *16*, 7889–7897.
- ²⁵Hait, D.; Head-Gordon, M. Excited State Orbital Optimization via Minimizing the Square of the Gradient: General Approach and Application to Singly and Doubly Excited States via Density Functional Theory. *J. Chem. Theory Comput.* **2020**, *16*, 1699–1710.
- ²⁶Hait, D.; Head-Gordon, M. Highly Accurate Prediction of Core Spectra of Molecules at Density Functional Theory Cost: Attaining Sub-electronvolt Error from a Restricted Open-Shell Kohn–Sham Approach. *J. Phys. Chem. Lett.* **2020**, *11*, 775–786.
- ²⁷Hait, D.; Head-Gordon, M. Orbital Optimized Density Functional Theory for Electronic Excited States. *J. Phys. Chem. Lett.* **2021**, *12*, 4517–4529.
- ²⁸Ye, H.-Z.; Welborn, M.; Rieke, N. D.; Van Voorhis, T. σ -SCF: A Direct Energy-Targeting Method to Mean-Field Excited States. *J. Chem. Phys.* **2017**, *147*, 214104.
- ²⁹Ye, H.-Z.; Van Voorhis, T. Half-Projected σ Self-Consistent Field For Electronic Excited States. *J. Chem. Theory Comput.* **2019**, *15*, 2954–2965.
- ³⁰Bagus, P. S. Self-Consistent-Field Wave Functions for Hole States of Some Ne-Like and Ar-Like Ions. *Phys. Rev.* **1965**, *139*, A619–A634.
- ³¹Hsu, H.-I.; Davidson, E. R.; Pitzer, R. M. An SCF Method for Hole States. *J. Chem. Phys.* **1976**, *65*, 609–613.
- ³²Naves de Brito, A.; Correia, N.; Svensson, S.; Ågren, H. A Theoretical Study of X-ray Photoelectron Spectra of Model Molecules for Polymethylmethacrylate. *J. Chem. Phys.* **1991**, *95*, 2965–2974.
- ³³Besley, N. A.; Gilbert, A. T. B.; Gill, P. M. W. Self-Consistent-Field Calculations of Core Excited States. *J. Chem. Phys.* **2009**, *130*, 124308.
- ³⁴Filatov, M.; Shaik, S. A Spin-Restricted Ensemble-Referenced Kohn–Sham Method and Its Application to Diradicaloid Situations. *Chemical Physics Letters* **1999**, *304*, 429–437.
- ³⁵Kowalczyk, T.; Tsuchimochi, T.; Chen, P.-T.; Top, L.; Van Voorhis, T. Excitation Energies and Stokes Shifts from a Restricted Open-Shell Kohn–Sham Approach. *J. Chem. Phys.* **2013**, *138*, 164101.
- ³⁶Kowalczyk, T.; Yost, S. R.; Voorhis, T. V. Assessment of the Δ SCF Density Functional Theory Approach for Electronic Excitations in Organic Dyes. *J. Chem. Phys.* **2011**, *134*, 054128.

- ³⁷Zhao, L.; Neuscammann, E. Density Functional Extension to Excited-State Mean-Field Theory. *J. Chem. Theory Comput.* **2020**, *16*, 164–178.
- ³⁸Levi, G.; Ivanov, A. V.; Jónsson, H. Variational Density Functional Calculations of Excited States via Direct Optimization. *J. Chem. Theory Comput.* **2020**, *16*, 6968–6982.
- ³⁹Kempfer-Robertson, E. M.; Haase, M. N.; Bersson, J. S.; Avdic, I.; Thompson, L. M. Role of Exact Exchange in Difference Projected Double-Hybrid Density Functional Theory for Treatment of Local, Charge Transfer, and Rydberg Excitations. *J. Phys. Chem. A* **2022**, *126*, 8058–8069.
- ⁴⁰Gilbert, A. T. B.; Besley, N. A.; Gill, P. M. W. Self-Consistent Field Calculations of Excited States Using the Maximum Overlap Method (MOM). *J. Phys. Chem. A* **2008**, *112*, 13164–13171.
- ⁴¹Barca, G. M. J.; Gilbert, A. T. B.; Gill, P. M. W. Simple Models for Difficult Electronic Excitations. *J. Chem. Theory Comput.* **2018**, *14*, 1501–1509.
- ⁴²Carter-Fenk, K.; Herbert, J. M. State-Targeted Energy Projection: A Simple and Robust Approach to Orbital Relaxation of Non-Aufbau Self-Consistent Field Solutions. *J. Chem. Theory Comput.* **2020**, *16*, 5067–5082.
- ⁴³Tran, L. N.; Shea, J. A. R.; Neuscammann, E. Tracking Excited States in Wave Function Optimization Using Density Matrices and Variational Principles. *J. Chem. Theory Comput.* **2019**, *15*, 4790–4803.
- ⁴⁴Tran, L. N.; Neuscammann, E. Improving Excited-State Potential Energy Surfaces via Optimal Orbital Shapes. *J. Phys. Chem. A* **2020**, *124*, 8273–8279.
- ⁴⁵Tran, L. N.; Neuscammann, E. Exploring Ligand-to-Metal Charge-Transfer States in the Photo-Ferrioxalate System Using Excited-State Specific Optimization. *J. Phys. Chem. Lett.* **2023**, *14*, 7454–7460.
- ⁴⁶Hanscam, R.; Neuscammann, E. Applying Generalized Variational Principles to Excited-State-Specific Complete Active Space Self-consistent Field Theory. *J. Chem. Theory Comput.* **2022**, *18*, 6608–6621.
- ⁴⁷Roos, B. O.; Andersson, K.; Fülcher, M. P. Towards an Accurate Molecular Orbital Theory for Excited States: The Benzene Molecule. *Chemical Physics Letters* **1992**, *192*, 5–13.
- ⁴⁸Boyn, J.-N.; Mazziotti, D. A. Elucidating the Molecular Orbital Dependence of the Total Electronic Energy in Multireference Problems. *J. Chem. Phys.* **2022**, *156*, 194104.
- ⁴⁹Shea, J. A. R.; Neuscammann, E. Communication: A Mean Field Platform for Excited State Quantum Chemistry. *J. Chem. Phys.* **2018**, *149*, 081101.
- ⁵⁰Shea, J. A. R.; Gwin, E.; Neuscammann, E. A Generalized Variational Principle with Applications to Excited State Mean Field Theory. *J. Chem. Theory Comput.* **2020**, *16*, 1526–1540.
- ⁵¹Hardikar, T. S.; Neuscammann, E. A Self-Consistent Field Formulation of Excited State Mean Field Theory. *J. Chem. Phys.* **2020**, *153*, 164108.
- ⁵²Liu, X.; Fatehi, S.; Shao, Y.; Veldkamp, B. S.; Subotnik, J. E. Communication: Adjusting Charge Transfer State Energies for Configuration Interaction Singles: Without Any Parameterization and with Minimal Cost. *J. Chem. Phys.* **2012**, *136*, 161101.
- ⁵³Kossoski, F.; Loos, P.-F. State-Specific Configuration Interaction for Excited States. *J. Chem. Theory Comput.* **2023**, *19*, 2258–2269.
- ⁵⁴Kossoski, F.; Loos, P.-F. Seniority and Hierarchy Configuration Interaction for Radicals and Excited States. *J. Chem. Theory Comput.* **2023**, *19*, 8654–8670.
- ⁵⁵Burton, H. G. A. Energy Landscape of State-Specific Electronic Structure Theory. *J. Chem. Theory Comput.* **2022**, *18*, 1512–1526.
- ⁵⁶Tsuchimochi, T. Double Configuration Interaction Singles: Scalable and Size-Intensive Approach for Orbital Relaxation in Excited States and Bond-Dissociation. *J. Chem. Phys.* **2024**, *161*, 241102.
- ⁵⁷Clune, R.; Neuscammann, E. An Excitation Matched Local Correlation Approach to Excited State Specific Perturbation Theory. *J. Chem. Phys.* **2025**, *163*, 094109.
- ⁵⁸Clune, R.; Shea, J. A. R.; Neuscammann, E. N5-Scaling Excited-State-Specific Perturbation Theory. *J. Chem. Theory Comput.* **2020**, *16*, 6132–6141.
- ⁵⁹Clune, R.; Shea, J. A. R.; Hardikar, T. S.; Tuckman, H.; Neuscammann, E. Studying Excited-State-Specific Perturbation Theory on the Thiel Set. *J. Chem. Phys.* **2023**, *158*, 224113.
- ⁶⁰Mayhall, N. J.; Raghavachari, K. Multiple Solutions to the Single-Reference CCSD Equations for NiH. *J. Chem. Theory Comput.* **2010**, *6*, 2714–2720.
- ⁶¹Zheng, X.; Cheng, L. Performance of Delta-Coupled-Cluster Methods for Calculations of Core-Ionization Energies of First-Row Elements. *J. Chem. Theory Comput.* **2019**, *15*, 4945–4955.
- ⁶²Lee, J.; Small, D. W.; Head-Gordon, M. Excited States via Coupled Cluster Theory without Equation-of-Motion Methods: Seeking Higher Roots with Application to Doubly Excited States and Double Core Hole States. *J. Chem. Phys.* **2019**, *151*, 214103.
- ⁶³Damour, Y.; Scemama, A.; Jacquemin, D.; Kossoski, F.; Loos, P.-F. State-Specific Coupled-Cluster Methods for Excited States. *J. Chem. Theory Comput.* **2024**, *20*, 4129–4145.
- ⁶⁴Kossoski, F.; Marie, A.; Scemama, A.; Caffarel, M.; Loos, P.-F. Excited States from State-Specific Orbital-Optimized Pair Coupled Cluster. *J. Chem. Theory Comput.* **2021**, *17*, 4756–4768.
- ⁶⁵Tuckman, H.; Neuscammann, E. Excited-State-Specific Pseudo-projected Coupled-Cluster Theory. *J. Chem. Theory Comput.* **2023**, *19*, 6160–6171.
- ⁶⁶Pineda Flores, S. D.; Neuscammann, E. Excited State Specific Multi-Slater Jastrow Wave Functions. *J. Phys. Chem. A* **2019**, *123*, 1487–1497.
- ⁶⁷Zhao, L.; Neuscammann, E. An Efficient Variational Principle for the Direct Optimization of Excited States. *J. Chem. Theory Comput.* **2016**, *12*, 3436–3440.
- ⁶⁸Robinson, P. J.; Pineda Flores, S. D.; Neuscammann, E. Excitation Variance Matching with Limited Configuration Interaction Expansions in Variational Monte Carlo. *J. Chem. Phys.* **2017**, *147*, 164114.
- ⁶⁹Blunt, N. S.; Neuscammann, E. Charge-Transfer Excited States: Seeking a Balanced and Efficient Wave Function Ansatz in Variational Monte Carlo. *J. Chem. Phys.* **2017**, *147*, 194101.
- ⁷⁰Shea, J. A. R.; Neuscammann, E. Size Consistent Excited States via Algorithmic Transformations between Variational Principles. *J. Chem. Theory Comput.* **2017**, *13*, 6078–6088.
- ⁷¹Garner, S. M.; Neuscammann, E. A Variational Monte Carlo Approach for Core Excitations. *J. Chem. Phys.* **2020**, *153*, 144108.
- ⁷²Otis, L.; Craig, I. M.; Neuscammann, E. A Hybrid Approach to Excited-State-Specific Variational Monte Carlo and Doubly Excited States. *J. Chem. Phys.* **2020**, *153*, 234105.
- ⁷³Shepard, S.; Panadés-Barrueta, R. L.; Moroni, S.; Scemama, A.; Filippi, C. Double Excitation Energies from Quantum Monte Carlo Using State-Specific Energy Optimization. *J. Chem. Theory Comput.* **2022**, *18*, 6722–6731.
- ⁷⁴Otis, L.; Neuscammann, E. Optimization Stability in Excited-State-Specific Variational Monte Carlo. *J. Chem. Theory Comput.* **2023**, *19*, 767–782.
- ⁷⁵Otis, L.; Neuscammann, E. A Promising Intersection of Excited-State-Specific Methods from Quantum Chemistry and Quantum Monte Carlo. *WIREs Comput. Mol. Sci.* **2023**, *13*, e1659.
- ⁷⁶Pathak, S.; Busemeyer, B.; Rodrigues, J. N. B.; Wagner, L. K. Excited States in Variational Monte Carlo Using a Penalty Method. *J. Chem. Phys.* **2021**, *154*, 034101.
- ⁷⁷Entwistle, M. T.; Schätzle, Z.; Erdman, P. A.; Hermann, J.; Noé, F. Electronic Excited States in Deep Variational Monte Carlo. *Nat Commun* **2023**, *14*, 274.
- ⁷⁸Quady, T. K.; Tuckman, H.; Neuscammann, E. Aufbau Suppressed Coupled Cluster As a Post-Linear-Response Method. *J. Chem. Theory Comput.* **2025**, *21*, 8843–8852.
- ⁷⁹Löwdin, P.-O. Quantum Theory of Many-Particle Systems. I. Physical Interpretations by Means of Density Matrices, Natu-

- ral Spin-Orbitals, and Convergence Problems in the Method of Configurational Interaction. *Phys. Rev.* **1955**, *97*, 1474–1489.
- ⁸⁰McWeeny, R. The Density Matrix in Many-Electron Quantum Mechanics I. Generalized Product Functions. Factorization and Physical Interpretation of the Density Matrices. *Proc. R. Soc. Lond. Ser. Math. Phys. Sci.* **1997**, *253*, 242–259.
- ⁸¹Daniilov, V. I.; Kruglyak, Y. A.; Pechenaya, V. I. The Electron Density-Bond Order Matrix and the Spin Density in the Restricted CI Method. *Theoret. Chim. Acta* **1969**, *13*, 288–296.
- ⁸²Szabo, A.; Ostlund, N. *Modern Quantum Chemistry*; Dover, 1996.
- ⁸³McWeeny, R.; Sutcliffe, B. T. *Methods of Molecular Quantum Mechanics*; Academic Press, 1969.
- ⁸⁴McWeeny, R. Some Recent Advances in Density Matrix Theory. *Rev. Mod. Phys.* **1960**, *32*, 335–369.
- ⁸⁵Jørgensen, P.; Simons, J. *Second Quantization-Based Methods in Quantum Chemistry*; Academic Press: New York, 1981.
- ⁸⁶Schmitt, M.; Meerts, L. *Frontiers and Advances in Molecular Spectroscopy*; Elsevier, 2018; pp 143–193.
- ⁸⁷Hellweg, A. The Accuracy of Dipole Moments from Spin-Component Scaled CC2 in Ground and Electronically Excited States. *J. Chem. Phys.* **2011**, *134*, 064103.
- ⁸⁸Tait, C. E.; Neuhaus, P.; Peeks, M. D.; Anderson, H. L.; Timmel, C. R. Transient EPR Reveals Triplet State Delocalization in a Series of Cyclic and Linear π -Conjugated Porphyrin Oligomers. *J. Am. Chem. Soc.* **2015**, *137*, 8284–8293.
- ⁸⁹Pulay, P. Analytical Derivatives, Forces, Force Constants, Molecular Geometries, and Related Response Properties in Electronic Structure Theory. *WIREs Comput. Mol. Sci.* **2014**, *4*, 169–181.
- ⁹⁰Yarkony, D. R. Diabolical Conical Intersections. *Rev. Mod. Phys.* **1996**, *68*, 985–1013.
- ⁹¹Furche, F.; Ahlrichs, R. Adiabatic Time-Dependent Density Functional Methods for Excited State Properties. *J. Chem. Phys.* **2002**, *117*, 7433–7447.
- ⁹²Salter, E. A.; Trucks, G. W.; Bartlett, R. J. Analytic Energy Derivatives in Many-Body Methods. I. First Derivatives. *J. Chem. Phys.* **1989**, *90*, 1752–1766.
- ⁹³Shavitt, I.; Bartlett, R. J. *Many-Body Methods in Chemistry and Physics: MBPT and Coupled-Cluster Theory*; Cambridge Molecular Science; Cambridge University Press: Cambridge, 2009.
- ⁹⁴Chrayteh, A.; Blondel, A.; Loos, P.-F.; Jacquemin, D. Mountaineering Strategy to Excited States: Highly Accurate Oscillator Strengths and Dipole Moments of Small Molecules. *J. Chem. Theory Comput.* **2021**, *17*, 416–438.
- ⁹⁵Sarkar, R.; Boggio-Pasqua, M.; Loos, P.-F.; Jacquemin, D. Benchmarking TD-DFT and Wave Function Methods for Oscillator Strengths and Excited-State Dipole Moments. *J. Chem. Theory Comput.* **2021**, *17*, 1117–1132.
- ⁹⁶Monkhorst, H. J. Calculation of properties with the coupled-cluster method. *Int. J. Quantum Chem.* **1977**, *12*, 421–432.
- ⁹⁷Dalgaard, E.; Monkhorst, H. J. Some Aspects of the Time-Dependent Coupled-Cluster Approach to Dynamic Response Functions. *Phys. Rev. A* **1983**, *28*, 1217–1222.
- ⁹⁸Sekino, H.; Bartlett, R. J. A Linear Response, Coupled-Cluster Theory for Excitation Energy. *Int. J. Quantum Chem.* **1984**, *26*, 255–265.
- ⁹⁹Koch, H.; Jørgensen, P. Coupled Cluster Response Functions. *J. Chem. Phys.* **1990**, *93*, 3333–3344.
- ¹⁰⁰Rico, R. J.; Head-Gordon, M. Single-Reference Theories of Molecular Excited States with Single and Double Substitutions. *Chemical Physics Letters* **1993**, *213*, 224–232.
- ¹⁰¹Koch, H.; Kobayashi, R.; Sanchez De Merás, A.; Jørgensen, P. Calculation of Size-Intensive Transition Moments from the Coupled Cluster Singles and Doubles Linear Response Function. *J. Chem. Phys.* **1994**, *100*, 4393–4400.
- ¹⁰²Sneskov, K.; Christiansen, O. Excited State Coupled Cluster Methods. *WIREs Comput. Mol. Sci.* **2012**, *2*, 566–584.
- ¹⁰³Schraivogel, T.; Cohen, A. J.; Alavi, A.; Kats, D. Transcorrelated Coupled Cluster Methods. *J. Chem. Phys.* **2021**, *155*, 191101.
- ¹⁰⁴Mörchen, M.; Baiardi, A.; Lesiuk, M.; Reiher, M. Non-Iterative Triples for Transcorrelated Coupled Cluster Theory. *J. Chem. Theory Comput.* **2025**, *21*, 1588–1601.
- ¹⁰⁵Arponen, J. S.; Bishop, R. F.; Pajanne, E. Extended Coupled-Cluster Method. I. Generalized Coherent Bosonization as a Mapping of Quantum Theory into Classical Hamiltonian Mechanics. *Phys. Rev. A* **1987**, *36*, 2519–2538.
- ¹⁰⁶Levchenko, S. V.; Wang, T.; Krylov, A. I. Analytic Gradients for the Spin-Conserving and Spin-Flipping Equation-of-Motion Coupled-Cluster Models with Single and Double Substitutions. *J. Chem. Phys.* **2005**, *122*, 224106.
- ¹⁰⁷Balková, A.; Bartlett, R. J. Coupled-Cluster Method for Open-Shell Singlet States. *Chemical Physics Letters* **1992**, *193*, 364–372.
- ¹⁰⁸Balková, A.; Bartlett, R. J. The Two-Determinant Coupled-Cluster Method for Electric Properties of Excited Electronic States: The Lowest $1 B$ 1 and $3 B$ 1 States of the Water Molecule. *J. Chem. Phys.* **1993**, *99*, 7907–7915.
- ¹⁰⁹Javed, Q.; Tuckman, H.; Neuscammen, E. Aufbau Suppressed Coupled Cluster Theory for Doubly Excited States. *arXiv.org* **2026**, 2601.20089.
- ¹¹⁰Salter, E. A.; Sekino, H.; Bartlett, R. J. Property Evaluation and Orbital Relaxation in Coupled Cluster Methods. *J. Chem. Phys.* **1987**, *87*, 502–509.
- ¹¹¹Bartlett, R. J.; Musiał, M. Coupled-Cluster Theory in Quantum Chemistry. *Rev. Mod. Phys.* **2007**, *79*, 291–352.
- ¹¹²Hodecker, M.; Rehn, D. R.; Dreuw, A.; Höfener, S. Similarities and Differences of the Lagrange Formalism and the Intermediate State Representation in the Treatment of Molecular Properties. *J. Chem. Phys.* **2019**, *150*, 164125.
- ¹¹³Arponen, J. Variational Principles and Linked-Cluster Exp S Expansions for Static and Dynamic Many-Body Problems. *Annals of Physics* **1983**, *151*, 311–382.
- ¹¹⁴Bachrach, S. M. *Reviews in Computational Chemistry*; John Wiley & Sons, Ltd, 1994; pp 171–228.
- ¹¹⁵Löwdin, P.-O. On the Non-Orthogonality Problem Connected with the Use of Atomic Wave Functions in the Theory of Molecules and Crystals. *J. Chem. Phys.* **1950**, *18*, 365–375.
- ¹¹⁶Contreras, R.; Domingo, L. R.; Silvi, B. *Encyclopedia of Physical Organic Chemistry*; John Wiley & Sons, Ltd, 2017; pp 1–114.
- ¹¹⁷North, S. C.; Jørgensen, K. R.; Pricetolstoy, J.; Wilson, A. K. Population Analysis and the Effects of Gaussian Basis Set Quality and Quantum Mechanical Approach: Main Group through Heavy Element Species. *Front Chem* **2023**, *11*, 1152500.
- ¹¹⁸Dreuw, A.; Head-Gordon, M. Single-Reference Ab Initio Methods for the Calculation of Excited States of Large Molecules. *Chem. Rev.* **2005**, *105*, 4009–4037.
- ¹¹⁹Fux, G. E.; Fowler-Wright, P.; Beckles, J.; Butler, E. P.; Eastham, P. R.; Gribben, D.; Keeling, J.; Kilda, D.; Kirton, P.; Lawrence, E. D. C.; Lovett, B. W.; O’Neill, E.; Strathearn, A.; De Wit, R. OQuPy: A Python Package to Efficiently Simulate Non-Markovian Open Quantum Systems with Process Tensors. *J. Chem. Phys.* **2024**, *161*, 124108.
- ¹²⁰Mardirossian, N.; Head-Gordon, M. ω B97X-V: A 10-Parameter, Range-Separated Hybrid, Generalized Gradient Approximation Density Functional with Nonlocal Correlation, Designed by a Survival-of-the-Fittest Strategy. *Phys. Chem. Chem. Phys.* **2014**, *16*, 9904.
- ¹²¹Epifanovsky, E. et al. Software for the Frontiers of Quantum Chemistry: An Overview of Developments in the Q-Chem 5 Package. *J. Chem. Phys.* **2021**, *155*, 084801.
- ¹²²Loos, P.-F.; Scemama, A.; Blondel, A.; Garniron, Y.; Cafarelli, M.; Jacquemin, D. A Mountaineering Strategy to Excited States: Highly Accurate Reference Energies and Benchmarks. *J. Chem. Theory Comput.* **2018**, *14*, 4360–4379.

- ¹²³Loos, P.-F.; Lipparini, F.; Boggio-Pasqua, M.; Scemama, A.; Jacquemin, D. A Mountaineering Strategy to Excited States: Highly Accurate Energies and Benchmarks for Medium Sized Molecules. *J. Chem. Theory Comput.* **2020**, *16*, 1711–1741.
- ¹²⁴Plasser, F.; Krylov, A. I.; Dreuw, A. Libwfa: Wavefunction Analysis Tools for Excited and Open-Shell Electronic States. *WIREs Comput. Mol. Sci.* **2022**, *12*, e1595.
- ¹²⁵Krylov, A. I. From Orbitals to Observables and Back. *J. Chem. Phys.* **2020**, *153*, 080901.
- ¹²⁶Plasser, F.; Wormit, M.; Dreuw, A. New Tools for the Systematic Analysis and Visualization of Electronic Excitations. I. Formalism. *J. Chem. Phys.* **2014**, *141*, 024106.
- ¹²⁷Plasser, F.; B pppler, S. A.; Wormit, M.; Dreuw, A. New Tools for the Systematic Analysis and Visualization of Electronic Excitations. II. Applications. *J. Chem. Phys.* **2014**, *141*, 024107.
- ¹²⁸Plasser, F.; Lischka, H. Analysis of Excitonic and Charge Transfer Interactions from Quantum Chemical Calculations. *J. Chem. Theory Comput.* **2012**, *8*, 2777–2789.
- ¹²⁹Mester, D.; Nagy, P. R.; Cs ka, J.; Gyevi-Nagy, L.; Szab , P. B.; Horv th, R. A.; Petrov, K.; H gely, B.; Lad czki, B.; Samu, G.; L rincz, B. D.; K llay, M. Overview of Developments in the MRCC Program System. *J. Phys. Chem. A* **2025**, *129*, 2086–2107.
- ¹³⁰K llay, M. et al. MRCC, a Quantum Chemical Program Suite. www.mrcc.hu.
- ¹³¹K llay, M.; Surj n, P. R. Higher Excitations in Coupled-Cluster Theory. *J. Chem. Phys.* **2001**, *115*, 2945–2954.
- ¹³²K llay, M.; Gauss, J.; Szalay, P. G. Analytic First Derivatives for General Coupled-Cluster and Configuration Interaction Models. *J. Chem. Phys.* **2003**, *119*, 2991–3004.
- ¹³³K llay, M.; Gauss, J. Calculation of Excited-State Properties Using General Coupled-Cluster and Configuration-Interaction Models. *J. Chem. Phys.* **2004**, *121*, 9257–9269.
- ¹³⁴Allouche, A.-R. Gabedit—A Graphical User Interface for Computational Chemistry Softwares. *J. Comput. Chem.* **2011**, *32*, 174–182.
- ¹³⁵Kozma, B.; Tajti, A.; Demoulin, B.; Izs k, R.; Nooijen, M.; Szalay, P. G. A New Benchmark Set for Excitation Energy of Charge Transfer States: Systematic Investigation of Coupled Cluster Type Methods. *J. Chem. Theory Comput.* **2020**, *16*, 4213–4225.

VIII. SUPPORTING INFORMATION

S1. RAW DATA

The attached .csv file contains all of the raw data from the various calculations used throughout this study with topics separated by worksheet. The first worksheet contains excitation energies (eV) for every iteration of the natural orbital refinement procedure using $\text{ASCC}^{(M,1)}$ and $\text{PLASCC}^{(M,1)}$ on the four different references: CIS, EOM-CCSD, TD-DFT/ ω B97X-V, and ESMF. For totally symmetric states, the “flipped” refers to the second (PL)ASCC solution. Values of N/A indicate that convergence was not achieved for the provided calculation. The reference values for all valence and Rydberg states are calculated at the exFCI level of theory except for thioformaldehyde’s 1^1A_2 , which is calculated at EOM-CCSDTQ. The reference values for all charge transfer states are calculated using EOM-CCSDT except for 3,5-difluoro-penta-2,3-dienamine, which is calculated using LR-CC3. The second worksheet contains the Mulliken and Löwdin population analyses results for EOM-CCSD, $\text{ASCC}^{(M,1)}$, and $\text{ASCC}^{(1,M)}$ on each of the charge transfer excitations. The third worksheet contains the Mulliken and Löwdin population analyses results for EOM-CCSD, $\text{ASCC}^{(M,1)}$, and $\text{ASCC}^{(1,M)}$ at each geometry in the water flyby system. The final worksheet contains the excitation energies (eV) and dipole moments (D) of the various versions of (PL)ASCC using each of the references alongside the values calculated with EOM-CCSD, (OU)LR-CCSD, and (OR)LR-CCSD. Reference excitation energies are at the exFCI level of theory, again except for thioformaldehyde’s 1^1A_2 , which is calculated at EOM-CCSDTQ. Reference dipole moments are calculated at (OR)LR-CCSDTQP for H_2O , H_2S , and CO and (OR)LR-CCSDTQ for formaldehyde and thioformaldehyde.

S2. CHARGE TRANSFER NATURAL ORBITAL REFINEMENT SUMMARY

TABLE S1. Diagnostics when performing natural orbital refinement on the ammonia-difluorine 2^1A_1 charge transfer excitation. N/A indicates that convergence could not be reached for the specific calculation or the previous calculation(s).

ASCC Variant	Reference	Diagnostic	Orbital Refinements				
			0	1	2	3	4
ASCC ^(M,1)	CIS	Energy	9.13	9.17	9.17	9.17	9.17
		Max $ T - T^{(0)} $	0.09	0.03	0.11	0.03	0.10
		Max $ \Lambda - \Lambda^{(0)} $	0.11	0.08	0.08	0.08	
ASCC ^(M,1)	EOM-CCSD	Energy	9.20	9.18	9.17	9.18	9.17
		Max $ T - T^{(0)} $	0.06	0.07	0.23	0.08	0.16
		Max $ \Lambda - \Lambda^{(0)} $	0.10	0.09	0.10	0.09	
ASCC ^(M,1)	ω B97X-V	Energy	9.14	9.17	9.17	9.17	9.17
		Max $ T - T^{(0)} $	0.09	0.03	0.13	0.03	0.11
		Max $ \Lambda - \Lambda^{(0)} $	0.11	0.08	0.08	0.08	
ASCC ^(M,1)	ESMF	Energy	9.17	9.17	9.17	9.17	9.17
		Max $ T - T^{(0)} $	0.03	0.20	0.07	0.16	0.03
		Max $ \Lambda - \Lambda^{(0)} $	0.08	0.09	0.09	0.08	
PLASCC ^(M,1)	CIS	Energy	9.28	9.38	9.38	9.38	9.38
		Max $ T - T^{(0)} $	0.09	0.03	0.03	0.03	0.03
		Max $ \Lambda - \Lambda^{(0)} $	0.09	0.07	0.07	0.07	
PLASCC ^(M,1)	EOM-CCSD	Energy	9.34	9.39	9.38	9.38	9.38
		Max $ T - T^{(0)} $	0.06	0.03	0.03	0.03	0.03
		Max $ \Lambda - \Lambda^{(0)} $	0.09	0.07	0.07	0.07	
PLASCC ^(M,1)	ω B97X-V	Energy	9.32	9.39	9.39	9.39	9.39
		Max $ T - T^{(0)} $	0.09	0.03	0.03	0.03	0.03
		Max $ \Lambda - \Lambda^{(0)} $	0.09	0.07	0.07	0.07	
PLASCC ^(M,1)	ESMF	Energy	9.37	9.39	9.39	9.39	9.39
		Max $ T - T^{(0)} $	0.03	0.03	0.03	0.03	0.03
		Max $ \Lambda - \Lambda^{(0)} $	0.07	0.07	0.07	0.07	

TABLE S2. Diagnostics when performing natural orbital refinement on the acetone-difluorine 3^1A charge transfer excitation. N/A indicates that convergence could not be reached for the specific calculation or the previous calculation(s).

ASCC Variant	Reference	Diagnostic	Orbital Refinements				
			0	1	2	3	4
ASCC ^(M,1)	CIS	Energy	5.77	5.83	5.80	5.75	5.21
		Max $ T - T^{(0)} $	0.14	0.07	0.15	0.41	0.34
		Max $ \Lambda - \Lambda^{(0)} $	0.20	0.11	0.13	0.16	
ASCC ^(M,1)	EOM-CCSD	Energy	5.84	5.50	4.66	4.44	4.40
		Max $ T - T^{(0)} $	0.13	0.43	0.17	0.19	0.19
		Max $ \Lambda - \Lambda^{(0)} $	0.28	0.39	0.19	0.17	
ASCC ^(M,1)	ω B97X-V	Energy	5.74	5.82	5.80	5.80	5.74
		Max $ T - T^{(0)} $	0.16	0.05	0.12	0.22	0.37
		Max $ \Lambda - \Lambda^{(0)} $	0.22	0.09	0.11	0.07	
ASCC ^(M,1)	ESMF	Energy	5.74	5.80	5.79	5.71	4.97
		Max $ T - T^{(0)} $	0.09	0.10	0.17	0.34	0.26
		Max $ \Lambda - \Lambda^{(0)} $	0.15	0.11	0.09	0.22	
PLASCC ^(M,1)	CIS	Energy	5.79	7.09	6.08	N/A	N/A
		Max $ T - T^{(0)} $	0.16	0.80	0.40	N/A	N/A
		Max $ \Lambda - \Lambda^{(0)} $	0.32	0.44	N/A	N/A	N/A
PLASCC ^(M,1)	EOM-CCSD	Energy	5.87	5.94	5.94	5.93	5.92
		Max $ T - T^{(0)} $	0.08	0.08	0.04	0.07	0.09
		Max $ \Lambda - \Lambda^{(0)} $	0.14	0.11	0.11	0.11	
PLASCC ^(M,1)	ω B97X-V	Energy	5.81	7.04	N/A	N/A	N/A
		Max $ T - T^{(0)} $	0.16	0.68	N/A	N/A	N/A
		Max $ \Lambda - \Lambda^{(0)} $	0.47	0.35	N/A	N/A	
PLASCC ^(M,1)	ESMF	Energy	5.85	5.96	5.96	5.96	5.96
		Max $ T - T^{(0)} $	0.10	0.04	0.04	0.03	0.04
		Max $ \Lambda - \Lambda^{(0)} $	0.12	0.08	0.08	0.08	

TABLE S3. Diagnostics when performing natural orbital refinement on the pyrazine-difluorine 2^1B_2 charge transfer excitation. N/A indicates that convergence could not be reached for the specific calculation or the previous calculation(s).

ASCC Variant	Reference	Diagnostic	Orbital Refinements				
			0	1	2	3	4
ASCC ^(M,1)	CIS	Energy	6.42	6.56	6.55	6.59	N/A
		Max $ T - T^{(0)} $	0.09	0.12	0.09	0.49	N/A
		Max $ \Lambda - \Lambda^{(0)} $	0.19	0.12	0.12	0.24	
ASCC ^(M,1)	EOM-CCSD	Energy	6.56	6.57	6.46	N/A	N/A
		Max $ T - T^{(0)} $	0.09	0.45	0.60	N/A	N/A
		Max $ \Lambda - \Lambda^{(0)} $	0.14	0.16	0.30	N/A	
ASCC ^(M,1)	ω B97X-V	Energy	6.48	6.56	6.55	6.61	6.29
		Max $ T - T^{(0)} $	0.09	0.14	0.12	0.49	0.98
		Max $ \Lambda - \Lambda^{(0)} $	0.18	0.12	0.12	0.26	
ASCC ^(M,1)	ESMF	Energy	6.51	6.56	6.56	6.56	6.53
		Max $ T - T^{(0)} $	0.09	0.09	0.09	0.17	0.33
		Max $ \Lambda - \Lambda^{(0)} $	0.13	0.12	0.12	0.14	
PLASCC ^(M,1)	CIS	Energy	6.33	6.61	6.72	N/A	N/A
		Max $ T - T^{(0)} $	0.09	0.19	0.19	N/A	N/A
		Max $ \Lambda - \Lambda^{(0)} $	0.16	0.24	0.27	N/A	
PLASCC ^(M,1)	EOM-CCSD	Energy	6.48	6.69	N/A	N/A	N/A
		Max $ T - T^{(0)} $	0.09	0.16	N/A	N/A	N/A
		Max $ \Lambda - \Lambda^{(0)} $	0.16	0.27	N/A	N/A	
PLASCC ^(M,1)	ω B97X-V	Energy	6.43	6.55	6.64	N/A	N/A
		Max $ T - T^{(0)} $	0.09	0.09	0.21	N/A	N/A
		Max $ \Lambda - \Lambda^{(0)} $	0.15	0.13	0.28	N/A	
PLASCC ^(M,1)	ESMF	Energy	6.47	6.56	6.74	N/A	N/A
		Max $ T - T^{(0)} $	0.09	0.11	0.22	N/A	N/A
		Max $ \Lambda - \Lambda^{(0)} $	0.12	0.15	0.34	N/A	

TABLE S4. Diagnostics when performing natural orbital refinement on the pyrazine-difluorine 2^1A_2 charge transfer excitation. N/A indicates that convergence could not be reached for the specific calculation or the previous calculation(s).

ASCC Variant	Reference	Diagnostic	Orbital Refinements				
			0	1	2	3	4
ASCC ^(M,1)	CIS	Energy	6.36	6.48	6.47	6.47	6.47
		Max $ T - T^{(0)} $	0.10	0.09	0.09	0.09	0.09
		Max $ \Lambda - \Lambda^{(0)} $	0.17	0.13	0.13	0.13	
ASCC ^(M,1)	EOM-CCSD	Energy	6.72	6.60	6.52	6.49	6.48
		Max $ T - T^{(0)} $	0.12	0.09	0.09	0.09	0.09
		Max $ \Lambda - \Lambda^{(0)} $	0.14	0.13	0.12	0.12	
ASCC ^(M,1)	ω B97X-V	Energy	6.37	6.47	6.46	6.47	6.47
		Max $ T - T^{(0)} $	0.12	0.09	0.09	0.09	0.09
		Max $ \Lambda - \Lambda^{(0)} $	0.19	0.13	0.13	0.13	
ASCC ^(M,1)	ESMF	Energy	6.41	6.47	6.46	6.47	6.47
		Max $ T - T^{(0)} $	0.09	0.09	0.09	0.09	0.09
		Max $ \Lambda - \Lambda^{(0)} $	0.15	0.13	0.13	0.13	
PLASCC ^(M,1)	CIS	Energy	6.36	6.73	6.60	6.67	N/A
		Max $ T - T^{(0)} $	0.21	0.11	0.27	0.12	N/A
		Max $ \Lambda - \Lambda^{(0)} $	0.20	0.32	0.30	0.46	
PLASCC ^(M,1)	EOM-CCSD	Energy	6.53	N/A	N/A	N/A	N/A
		Max $ T - T^{(0)} $	0.17	N/A	N/A	N/A	N/A
		Max $ \Lambda - \Lambda^{(0)} $	0.35	N/A	N/A	N/A	
PLASCC ^(M,1)	ω B97X-V	Energy	6.62	N/A	N/A	N/A	N/A
		Max $ T - T^{(0)} $	0.32	N/A	N/A	N/A	N/A
		Max $ \Lambda - \Lambda^{(0)} $	0.16	N/A	N/A	N/A	
PLASCC ^(M,1)	ESMF	Energy	6.58	6.69	N/A	N/A	N/A
		Max $ T - T^{(0)} $	0.29	0.10	N/A	N/A	N/A
		Max $ \Lambda - \Lambda^{(0)} $	0.24	0.91	N/A	N/A	

TABLE S5. Diagnostics when performing natural orbital refinement on the ammonia-oxygendifluorine 4^1A charge transfer excitation. The CIS reference was determined to be 2-CSF. Elsewhere, N/A indicates that convergence could not be reached for the specific calculation or the previous calculation(s).

ASCC Variant	Reference	Diagnostic	Orbital Refinements				
			0	1	2	3	4
ASCC ^(M,1)	CIS	Energy	N/A	N/A	N/A	N/A	N/A
		Max $ T - T^{(0)} $	N/A	N/A	N/A	N/A	N/A
		Max $ \Lambda - \Lambda^{(0)} $	N/A	N/A	N/A	N/A	
ASCC ^(M,1)	EOM-CCSD	Energy	7.08	6.99	6.98	6.97	6.97
		Max $ T - T^{(0)} $	0.15	0.07	0.07	0.07	0.07
		Max $ \Lambda - \Lambda^{(0)} $	0.15	0.09	0.09	0.09	
ASCC ^(M,1)	ω B97X-V	Energy	6.95	6.94	6.94	6.94	6.94
		Max $ T - T^{(0)} $	0.10	0.07	0.07	0.07	0.07
		Max $ \Lambda - \Lambda^{(0)} $	0.17	0.10	0.09	0.09	
ASCC ^(M,1)	ESMF	Energy	6.95	6.98	6.97	6.97	6.97
		Max $ T - T^{(0)} $	0.18	0.18	0.07	0.07	0.07
		Max $ \Lambda - \Lambda^{(0)} $	0.13	0.10	0.08	0.08	
PLASCC ^(M,1)	CIS	Energy	N/A	N/A	N/A	N/A	N/A
		Max $ T - T^{(0)} $	N/A	N/A	N/A	N/A	N/A
		Max $ \Lambda - \Lambda^{(0)} $	N/A	N/A	N/A	N/A	N/A
PLASCC ^(M,1)	EOM-CCSD	Energy	6.94	N/A	N/A	N/A	N/A
		Max $ T - T^{(0)} $	0.26	N/A	N/A	N/A	N/A
		Max $ \Lambda - \Lambda^{(0)} $	1.15	N/A	N/A	N/A	
PLASCC ^(M,1)	ω B97X-V	Energy	6.97	7.19	N/A	N/A	N/A
		Max $ T - T^{(0)} $	0.54	1.06	N/A	N/A	N/A
		Max $ \Lambda - \Lambda^{(0)} $	0.30	0.38	N/A	N/A	
PLASCC ^(M,1)	ESMF	Energy	7.01	7.06	N/A	N/A	N/A
		Max $ T - T^{(0)} $	0.09	0.19	N/A	N/A	N/A
		Max $ \Lambda - \Lambda^{(0)} $	0.09	N/A	N/A	N/A	

TABLE S6. Diagnostics when performing natural orbital refinement on the tetrafluoroethylene-ethylene 5^1B_1 charge transfer excitation. N/A indicates that convergence could not be reached for the specific calculation or the previous calculation(s).

ASCC Variant	Reference	Diagnostic	Orbital Refinements				
			0	1	2	3	4
ASCC ^(M,1)	CIS	Energy	10.55	N/A	N/A	N/A	N/A
		Max $ T - T^{(0)} $	0.17	N/A	N/A	N/A	N/A
		Max $ \Lambda - \Lambda^{(0)} $	0.22	N/A	N/A	N/A	
ASCC ^(M,1)	EOM-CCSD	Energy	10.69	10.66	10.71	10.66	10.27
		Max $ T - T^{(0)} $	0.10	0.30	0.35	0.34	0.25
		Max $ \Lambda - \Lambda^{(0)} $	0.16	0.19	0.25	0.58	
ASCC ^(M,1)	ω B97X-V	Energy	10.31	9.78	9.56	9.46	9.40
		Max $ T - T^{(0)} $	0.39	0.15	0.14	0.14	0.14
		Max $ \Lambda - \Lambda^{(0)} $	0.49	0.15	0.13	0.13	
ASCC ^(M,1)	ESMF	Energy	10.39	11.18	-0.02	-0.03	-0.03
		Max $ T - T^{(0)} $	0.44	0.54	0.42	0.42	0.42
		Max $ \Lambda - \Lambda^{(0)} $	0.50	1.26	0.88	0.65	
PLASCC ^(M,1)	CIS	Energy	10.53	10.79	10.78	10.78	10.78
		Max $ T - T^{(0)} $	0.10	0.03	0.03	0.03	0.03
		Max $ \Lambda - \Lambda^{(0)} $	0.12	0.09	0.09	0.09	
PLASCC ^(M,1)	EOM-CCSD	Energy	10.68	10.78	10.78	10.78	10.78
		Max $ T - T^{(0)} $	0.05	0.03	0.03	0.03	0.03
		Max $ \Lambda - \Lambda^{(0)} $	0.10	0.09	0.09	0.09	
PLASCC ^(M,1)	ω B97X-V	Energy	10.57	10.75	10.78	10.78	10.78
		Max $ T - T^{(0)} $	0.16	0.11	0.07	0.04	0.03
		Max $ \Lambda - \Lambda^{(0)} $	0.25	0.13	0.11	0.10	
PLASCC ^(M,1)	ESMF	Energy	10.58	10.78	10.78	10.78	10.78
		Max $ T - T^{(0)} $	0.11	0.05	0.03	0.03	0.03
		Max $ \Lambda - \Lambda^{(0)} $	0.13	0.10	0.09	0.09	

TABLE S7. Diagnostics when performing natural orbital refinement on the 3,5-difluoro-penta-2,4-dienamine 1^1A_1 charge transfer excitation. N/A indicates that convergence could not be reached for the specific calculation or the previous calculation(s).

ASCC Variant	Reference	Diagnostic	Orbital Refinements				
			0	1	2	3	4
ASCC ^(M,1)	CIS	Energy	7.07	6.96	6.76	6.34	6.24
		Max $ T - T^{(0)} $	0.30	0.13	0.26	0.24	0.23
		Max $ \Lambda - \Lambda^{(0)} $	0.31	0.19	0.49	0.18	
ASCC ^(M,1)	EOM-CCSD	Energy	6.96	6.94	6.85	6.45	6.26
		Max $ T - T^{(0)} $	0.26	0.10	0.22	0.25	0.23
		Max $ \Lambda - \Lambda^{(0)} $	0.23	0.14	0.40	0.27	
ASCC ^(M,1)	ω B97X-V	Energy	6.98	6.94	6.85	6.45	6.26
		Max $ T - T^{(0)} $	0.30	0.10	0.22	0.25	0.24
		Max $ \Lambda - \Lambda^{(0)} $	0.27	0.13	0.40	0.24	
ASCC ^(M,1)	ESMF	Energy	6.84	6.89	6.88	6.87	6.87
		Max $ T - T^{(0)} $	0.09	0.05	0.06	0.09	0.13
		Max $ \Lambda - \Lambda^{(0)} $	0.08	0.09	0.10	0.13	
PLASCC ^(M,1)	CIS	Energy	N/A	N/A	N/A	N/A	N/A
		Max $ T - T^{(0)} $	N/A	N/A	N/A	N/A	N/A
		Max $ \Lambda - \Lambda^{(0)} $	N/A	N/A	N/A	N/A	
PLASCC ^(M,1)	EOM-CCSD	Energy	6.74	6.67	N/A	N/A	N/A
		Max $ T - T^{(0)} $	0.16	0.22	N/A	N/A	N/A
		Max $ \Lambda - \Lambda^{(0)} $	0.31	0.42	N/A	N/A	
PLASCC ^(M,1)	ω B97X-V	Energy	6.82	N/A	N/A	N/A	N/A
		Max $ T - T^{(0)} $	0.20	N/A	N/A	N/A	N/A
		Max $ \Lambda - \Lambda^{(0)} $	0.34	N/A	N/A	N/A	
PLASCC ^(M,1)	ESMF	Energy	6.76	6.84	6.67	N/A	N/A
		Max $ T - T^{(0)} $	0.12	0.05	0.30	N/A	N/A
		Max $ \Lambda - \Lambda^{(0)} $	0.17	0.11	1.00	N/A	